Modeling neutrino-nucleus interaction at intermediate energies

Raúl González Jiménez

**Department of Physics and Astronomy,
Ghent University, Belgium**

*The 19th International Workshop on Neutrinos from Accelators (NuFact17),
Uppsala, Sweden, 25-30 September, 2017*

Ghent group

Natalie Jachowicz

Nils Van Dessel

Kajetan Niewczas

Jannes Nys

Tom Van Cuyck

Vishvas Pandey

Alexis Nikolakopoulos

Outline

I Introduction

II QE (mean-field vs plane waves)

III Low-excitation energies: CRPA

IV 2p2h processes

IV Single-pion production

VI Conclusions

What we know from (e,e')

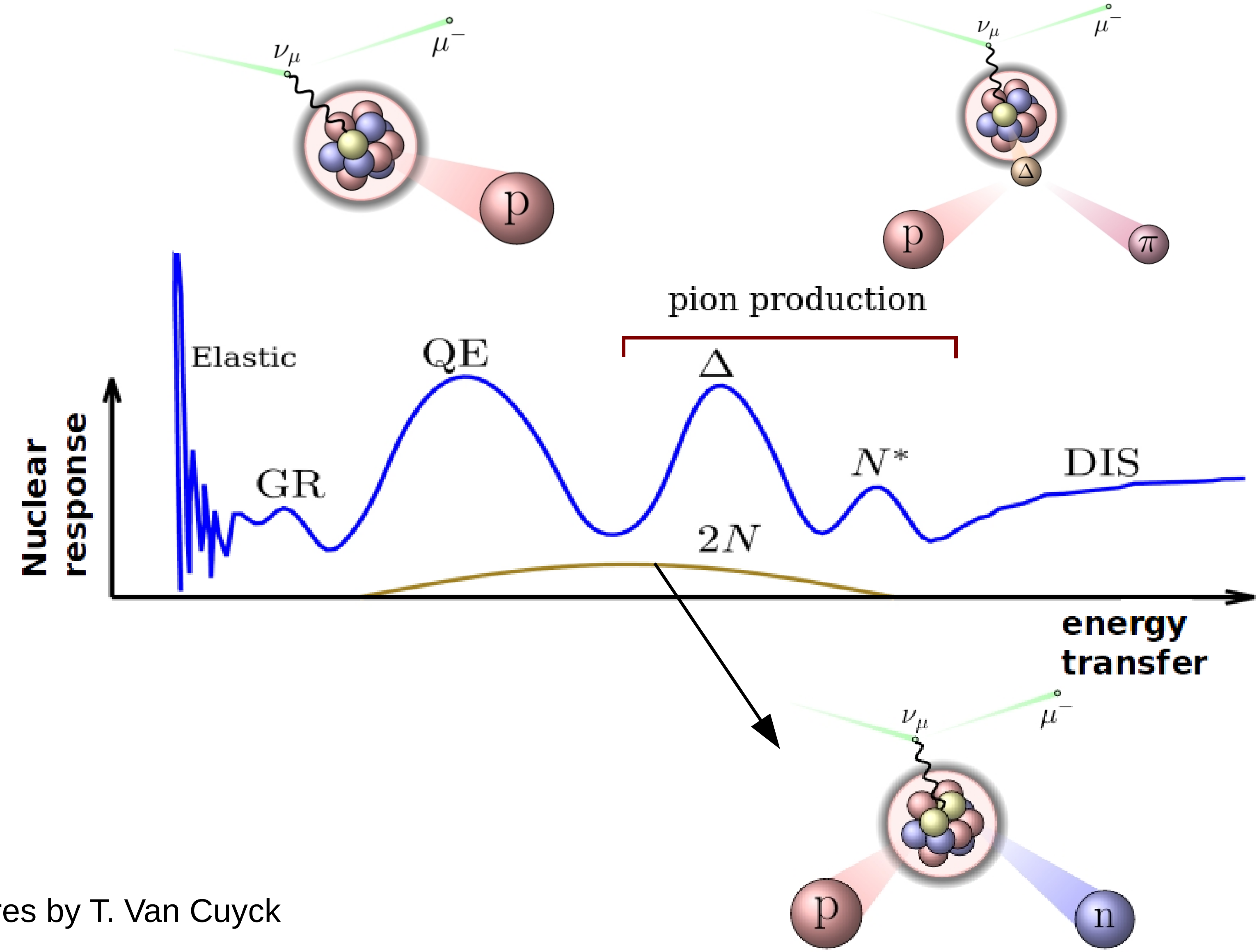

Figures by T. Van Cuyck

What we know from (e,e')

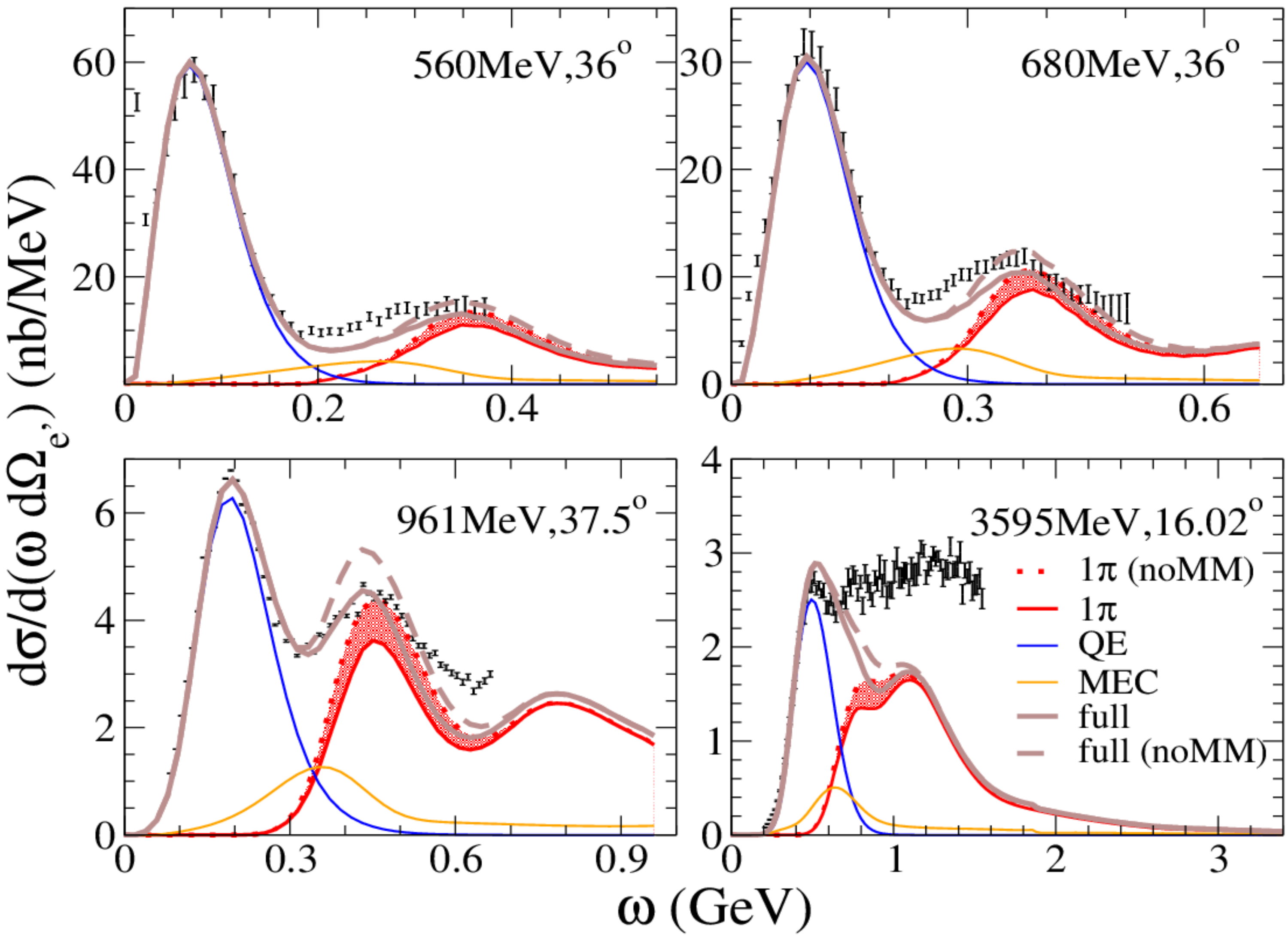

QE (SuSAv2): RGJ et al., PRC 90, 035501 (2014)

MEC: Megias et al., PRD 91, 073004 (2015)

1pion: RGJ et al., JPS Conf.Proc. 12, 010047 (2016); PRD 95, 113007 (2017)

Quasielastic scattering

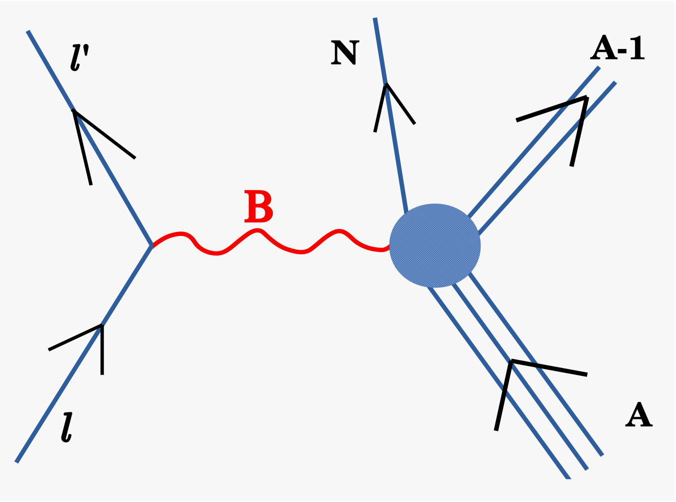

Impulse approximation

$$J^{\mu}_{had} = \langle N, A-1 | \hat{\mathcal{O}}^{\mu}_{many\text{-}body} | A \rangle$$

Impulse Approximation

$$J^{\mu}_{had} = \sum_{i}^{A} \int \mathbf{dr}\, \overline{\Psi}_F(\mathbf{r})\, \hat{\mathcal{O}}^{\mu}_{one\text{-}body}\, \Psi_B(\mathbf{r})\; e^{i\mathbf{q}\cdot\mathbf{r}}$$

where $\hat{\mathcal{O}}^{\mu}_{one\text{-}body} = F_1 \gamma^{\mu} + i \dfrac{F_2}{2M_N} \sigma^{\mu\alpha} Q_{\alpha}$

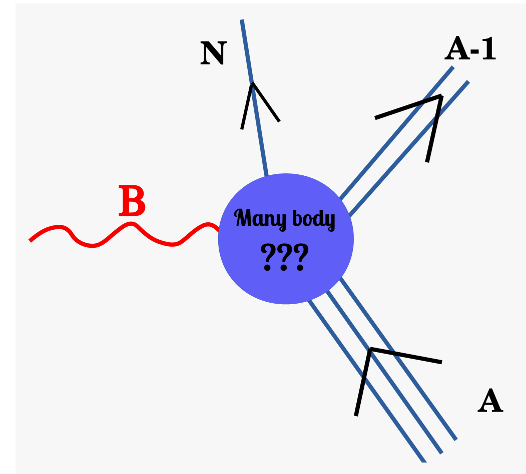

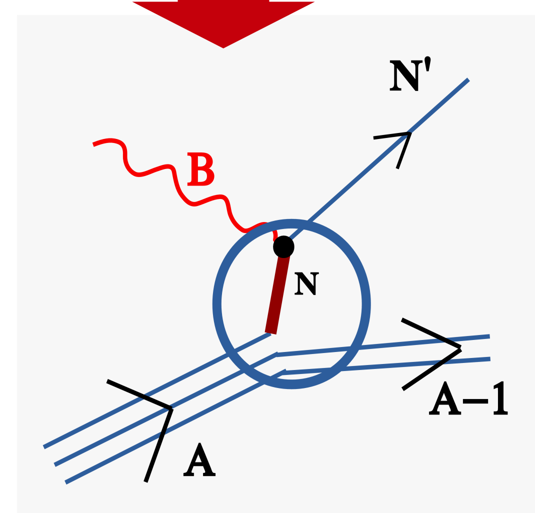

Impulse approximation

$$J^{\mu}_{had} = \langle N, A-1 | \hat{\mathcal{O}}^{\mu}_{many\text{-}body} | A \rangle$$

Impulse Approximation

Mean-field wave functions

$$J^{\mu}_{had} = \sum_{i}^{A} \int d\mathbf{r}\, \overline{\Psi}_F(\mathbf{r})\, \hat{\mathcal{O}}^{\mu}_{one\text{-}body}\, \Psi_B(\mathbf{r})\, e^{i\mathbf{q}\cdot\mathbf{r}}$$

where $$\hat{\mathcal{O}}^{\mu}_{one\text{-}body} = F_1 \gamma^{\mu} + i \frac{F_2}{2M_N} \sigma^{\mu\alpha} Q_{\alpha}$$

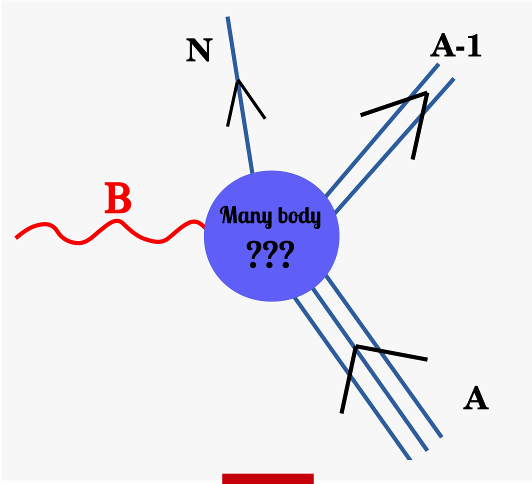

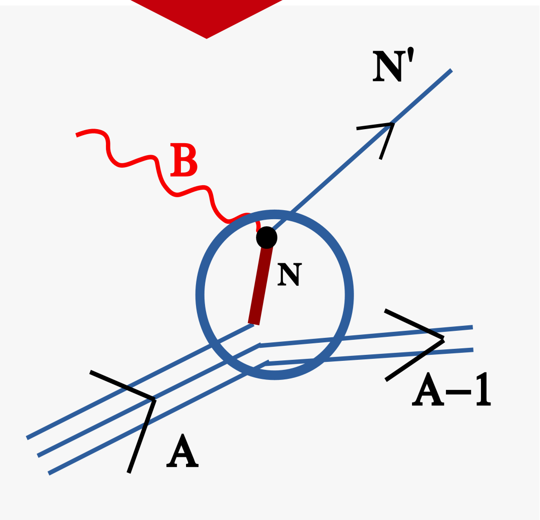

Nuclear Model (HF)

Figures by T. Van Cuyck

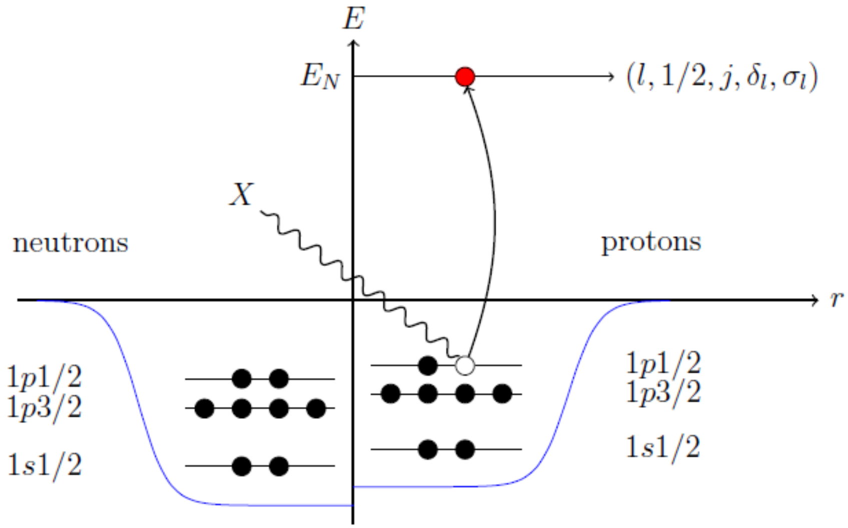

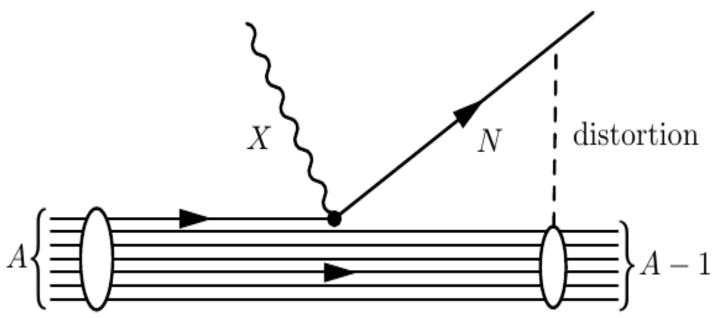

I) Ground state nucleus is a shell model:

➔ The mean field and wave functions are calculated with a Hartree-Fock (HF) approximation using an effective Skyrme NN force (SkE2).

➔ Binding energies, Fermi motion, nuclear structure.

II) Continuum wave functions are calculated using the same mean-field potential:

➔ The residual nucleus influence the knocked out nucleon (distorted waves).

Mean-field vs plane waves

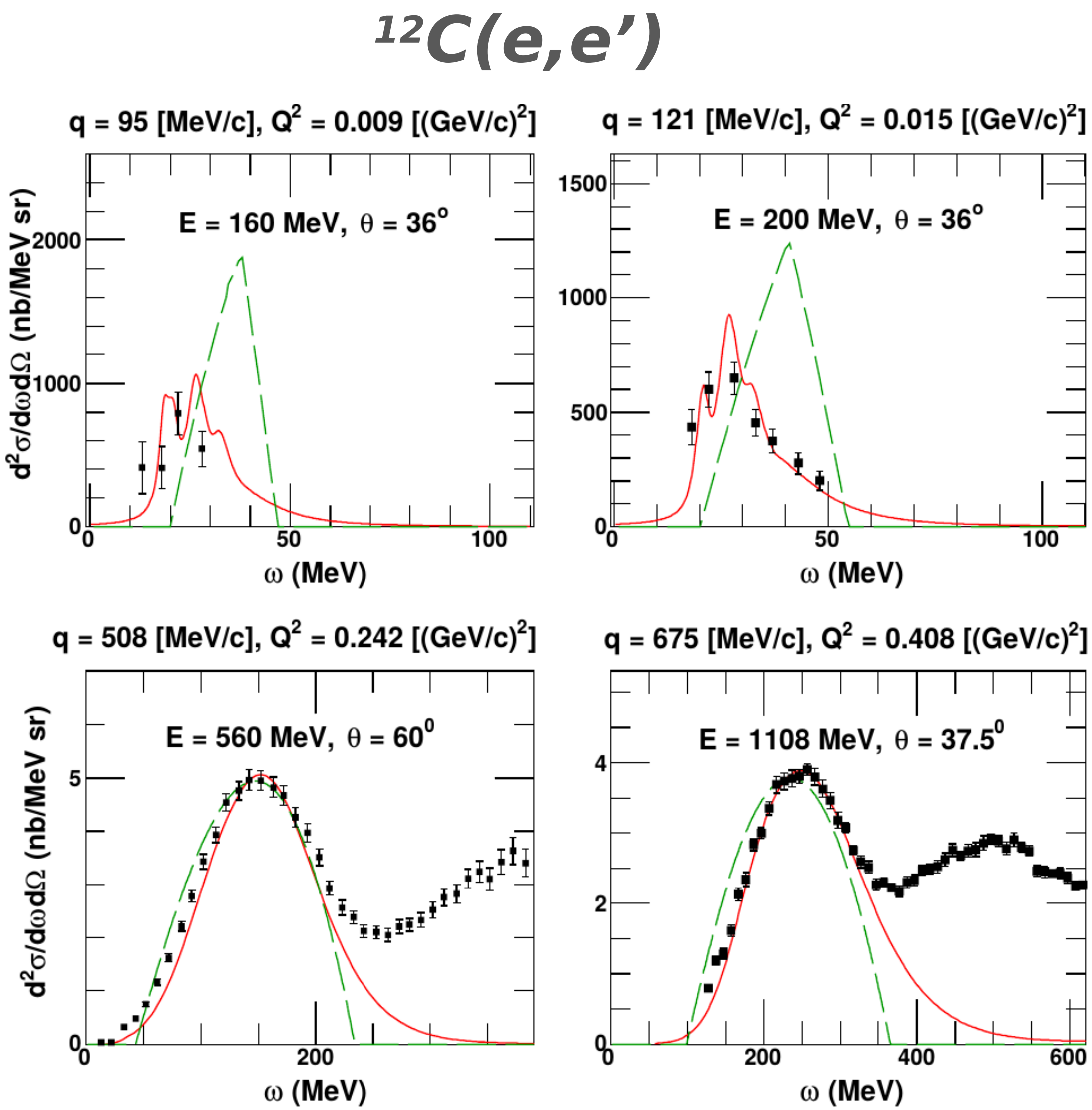

Red line: CRPA [V. Pandey PhD Thesis; PRC 92, 024606 (2015)]

Green line: Relativistic Fermi Gas with Pauli blocking [Amaro et al., PRC 71, 065501 (2005); RGJ et al., PRC 90, 035501 (2014)]

Nuclear Model (RMF)

Relativistic mean-field (RMF) model:

✔ <u>Same philosophy:</u> mean-field wave functions

✔ <u>Completely different approach:</u> fully relativistic (Dirac vs Schrödinger)

✔ <u>Similar results:</u> excellent agreement with QE data

✔ <u>Same conclusions:</u> mean-field wave functions in both initial and final nucleon are essential

Mean-field vs plane waves

Intermediate energies (typical QE regime)

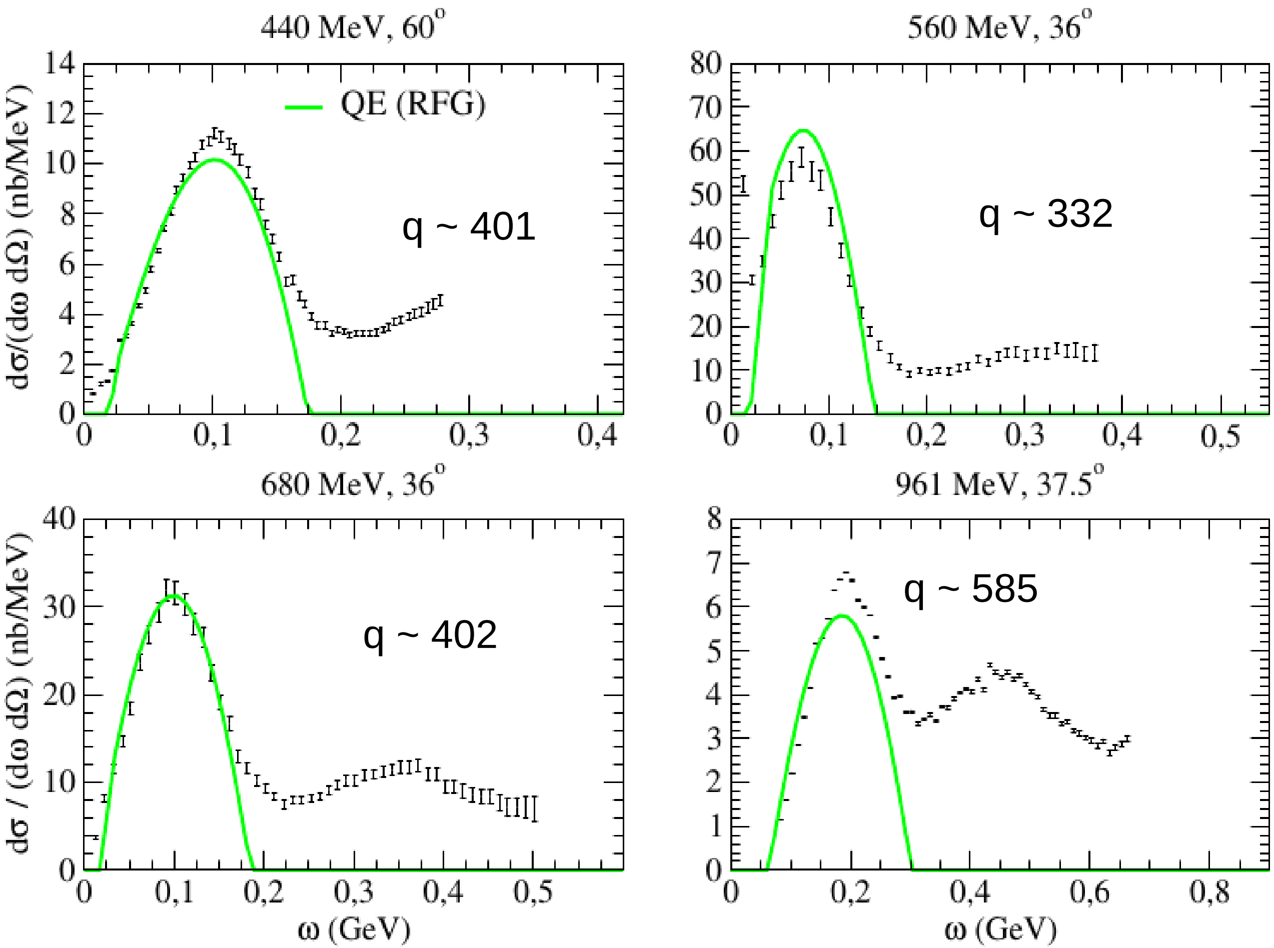

Mean-field vs plane waves

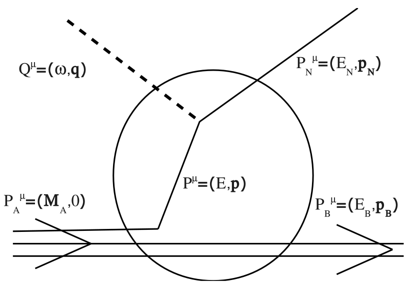

RPWIA: Scattered nucleon wf is described as a Dirac plane wave.

$$[-i\boldsymbol{\alpha}\cdot\boldsymbol{\nabla}+V(r)+\beta(M+S(r)]\Psi_i(\boldsymbol{r})=E_i\Psi_i(\boldsymbol{r})$$

$$J^\mu_{had}=\sum_i^A\int d\mathbf{r}\,\overline{\Psi}_F(\mathbf{r})\,\hat{\mathcal{O}}^\mu_{one\text{-}body}\,\Psi_B(\mathbf{r})\,e^{i\mathbf{q}\cdot\mathbf{r}}$$

Intermediate energies (typical QE regime)

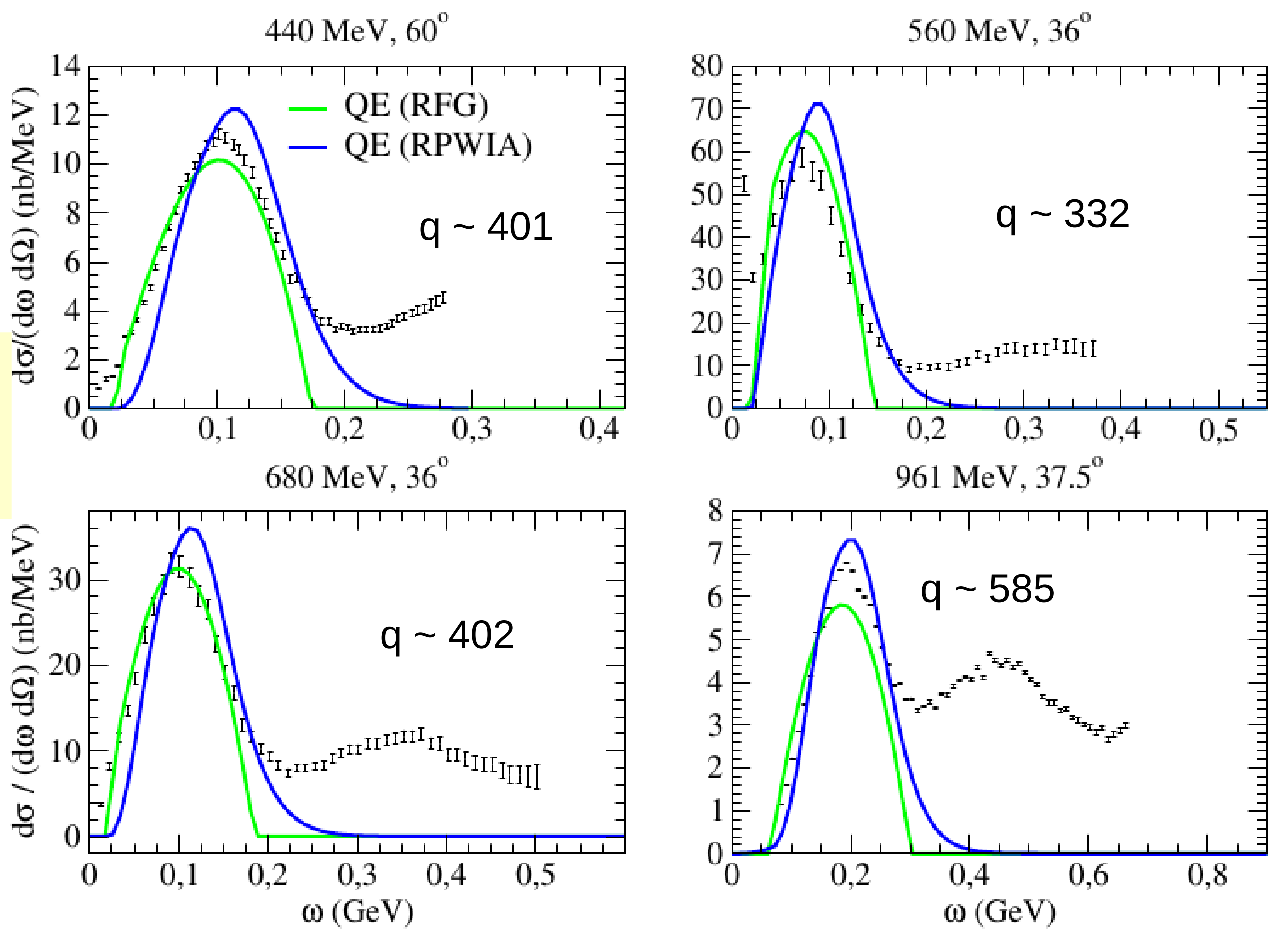

Mean-field vs plane waves

$$[-i\boldsymbol{\alpha}\cdot\boldsymbol{\nabla} + V(r) + \beta(M + S(r)]\Psi_i(\boldsymbol{r}) = E_i\Psi_i(\boldsymbol{r})$$

$$J^{\mu}_{had} = \sum_{i}^{A} \int d\mathbf{r}\,\overline{\Psi}_F(\mathbf{r})\,\hat{\mathcal{O}}^{\mu}_{one\text{-}body}\,\Psi_B(\mathbf{r})\,e^{i\mathbf{q}\cdot\mathbf{r}}$$

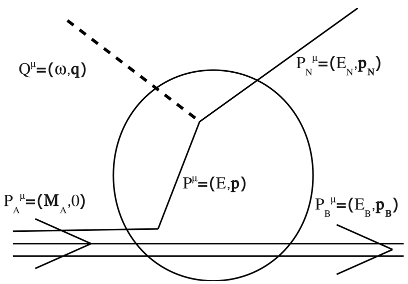

RPWIA: Scattered nucleon wf is described as a Dirac plane wave.

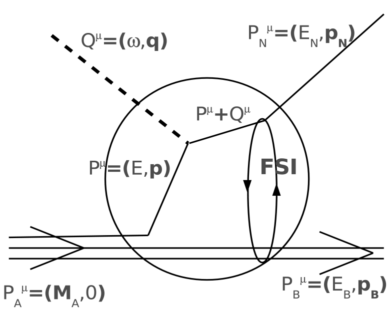

RMF-FSI: Scattered nucleon wf is solution of Dirac eq. in presence of the same potentials used to describe the bound nucleon wf.

Intermediate energies (typical QE regime)

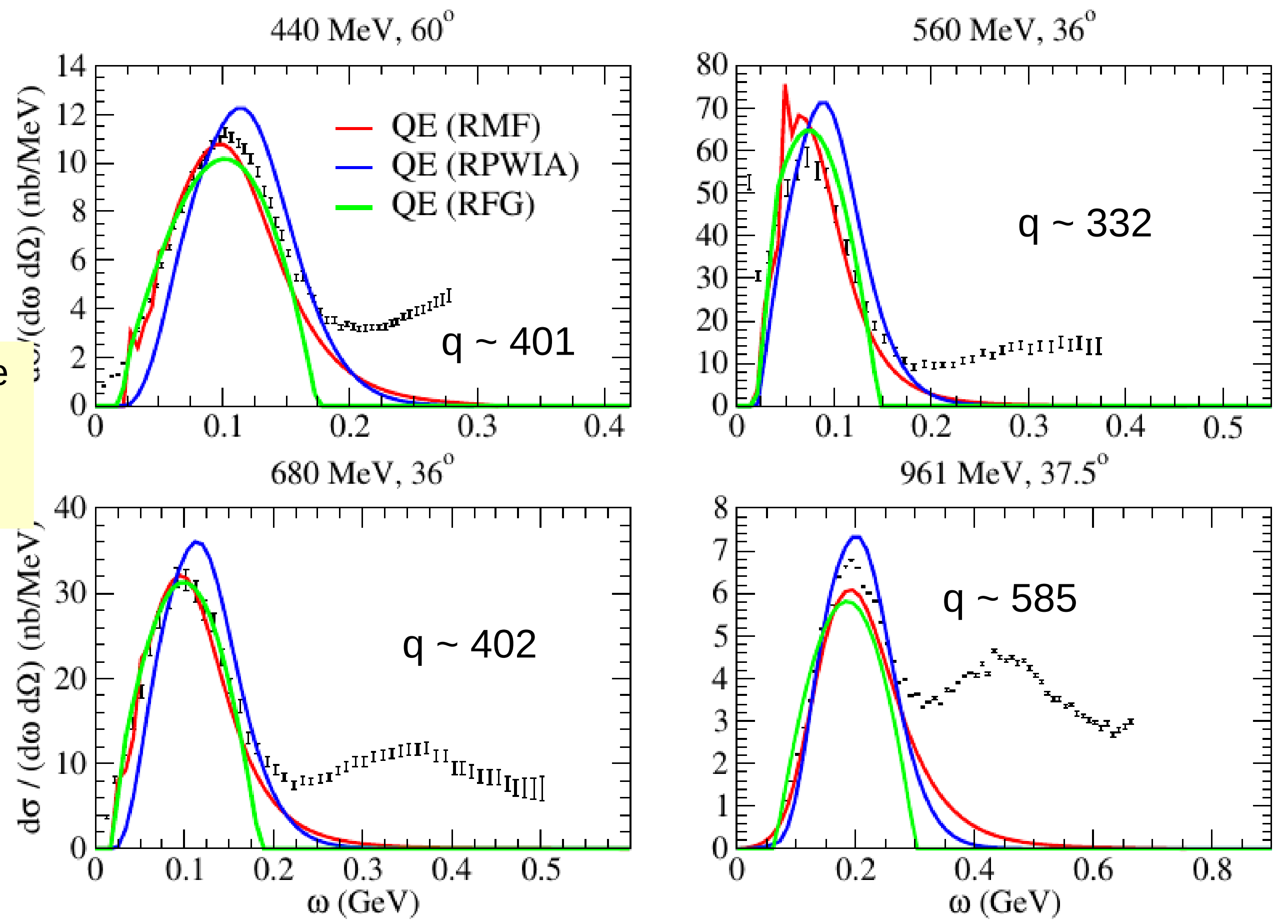

R. González-Jiménez Ghent University

Mean-field vs plane waves

$$[-i\boldsymbol{\alpha}\cdot\boldsymbol{\nabla} + V(r) + \beta(M + S(r)]\Psi_i(\boldsymbol{r}) = E_i\Psi_i(\boldsymbol{r})$$

$$J^{\mu}_{had} = \sum_{i}^{A} \int \mathrm{d}\mathbf{r}\, \overline{\Psi}_F(\mathbf{r})\, \hat{\mathcal{O}}^{\mu}_{one\text{-}body}\, \Psi_B(\mathbf{r})\, e^{i\mathbf{q}\cdot\mathbf{r}}$$

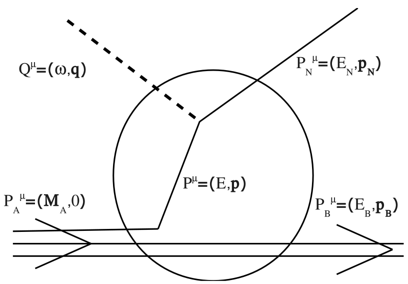

RPWIA: Scattered nucleon wf is described as a Dirac plane wave.

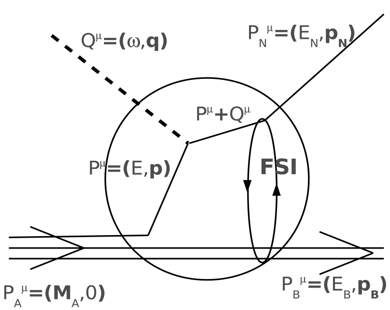

RMF-FSI: Scattered nucleon wf is solution of Dirac eq. in presence of the same potentials used to describe the bound nucleon wf.

Low energies

High energies

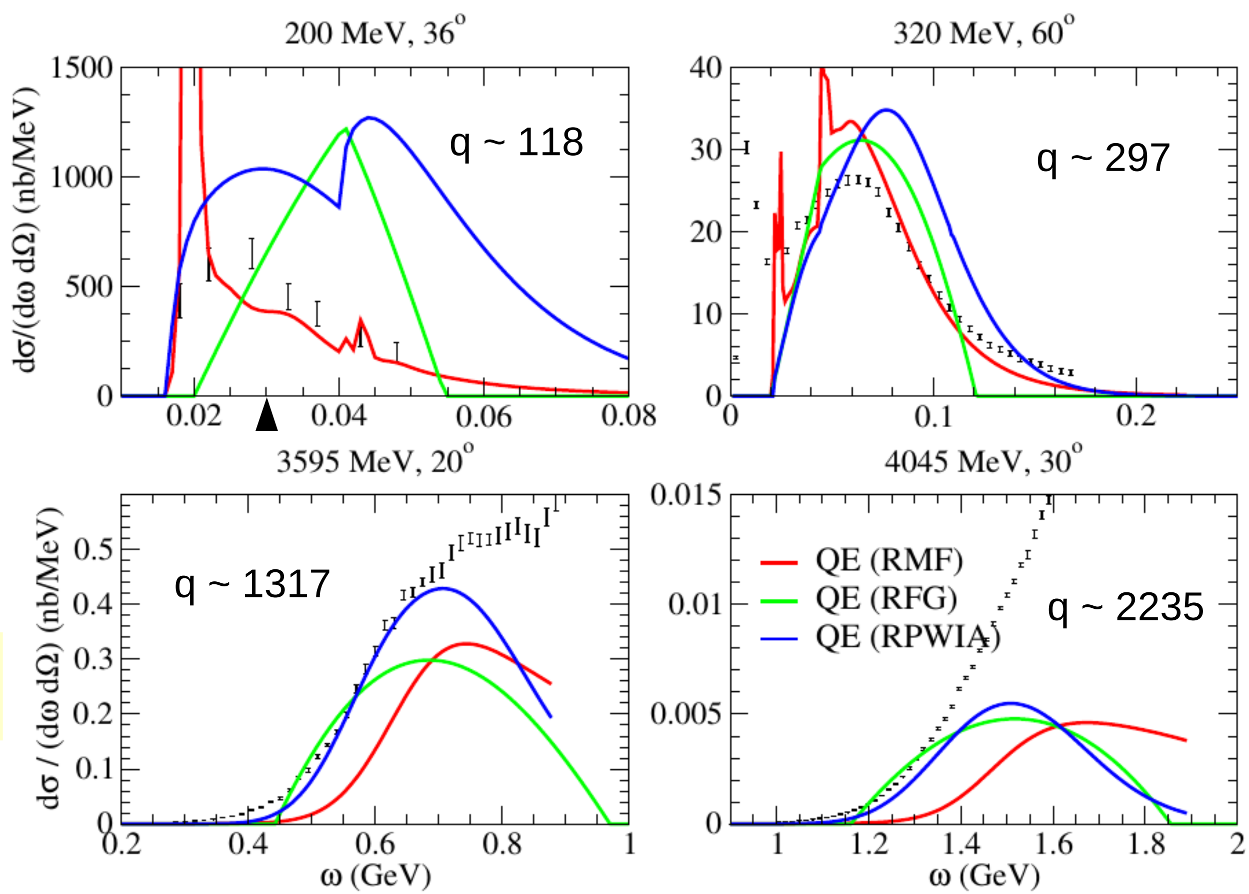

Long-range correlations: CRPA model

+ Long-range correlations between the nucleons are introduce through a **continuum Random Phase Approximation** (CRPA).

+ RPA equations are solved using a Green's function approach.

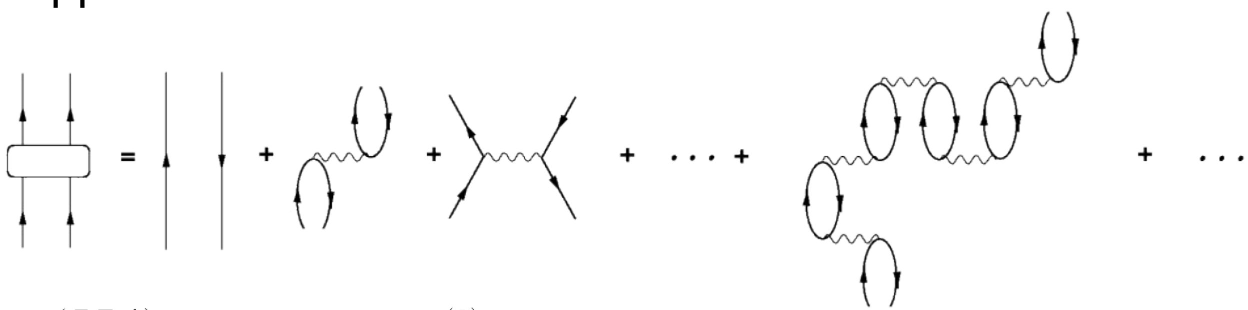

$$\Pi^{(RPA)}(x_1, x_2; \omega) = \Pi^{(0)}(x_1, x_2; \omega) + \frac{1}{\hbar} \int dx \int dx' \, \Pi^{(0)}(x_1, x; \omega) \, \widetilde{V}(x, x') \, \Pi^{(RPA)}(x', x_2; \omega)$$

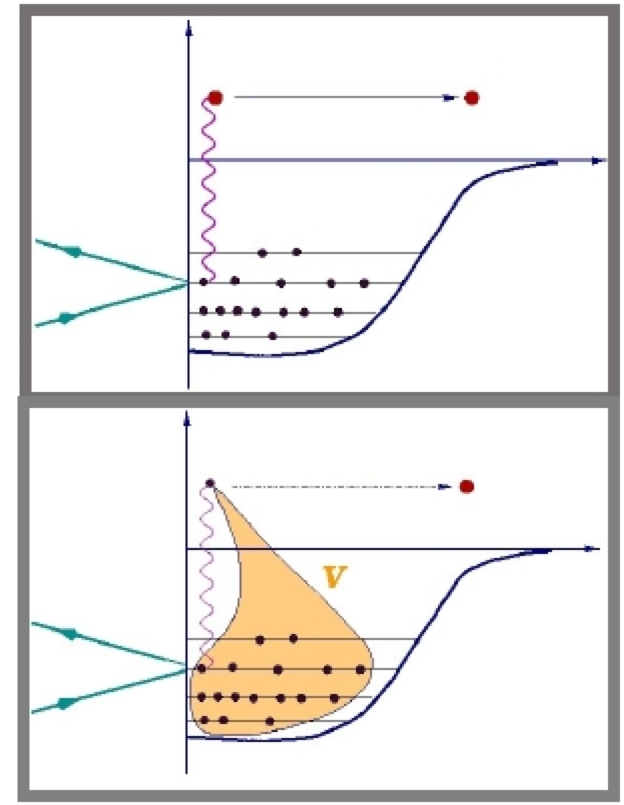

Excitations are obtained as linear combinations of different particle-hole configurations.

$$|\Psi_{RPA}\rangle = \sum_{c} \left\{ X_{(\Psi,C)} \left| ph^{-1} \right\rangle - Y_{(\Psi,C)} \left| hp^{-1} \right\rangle \right\}$$

Long-range correlations: CRPA model

$^{12}C(e, e')$

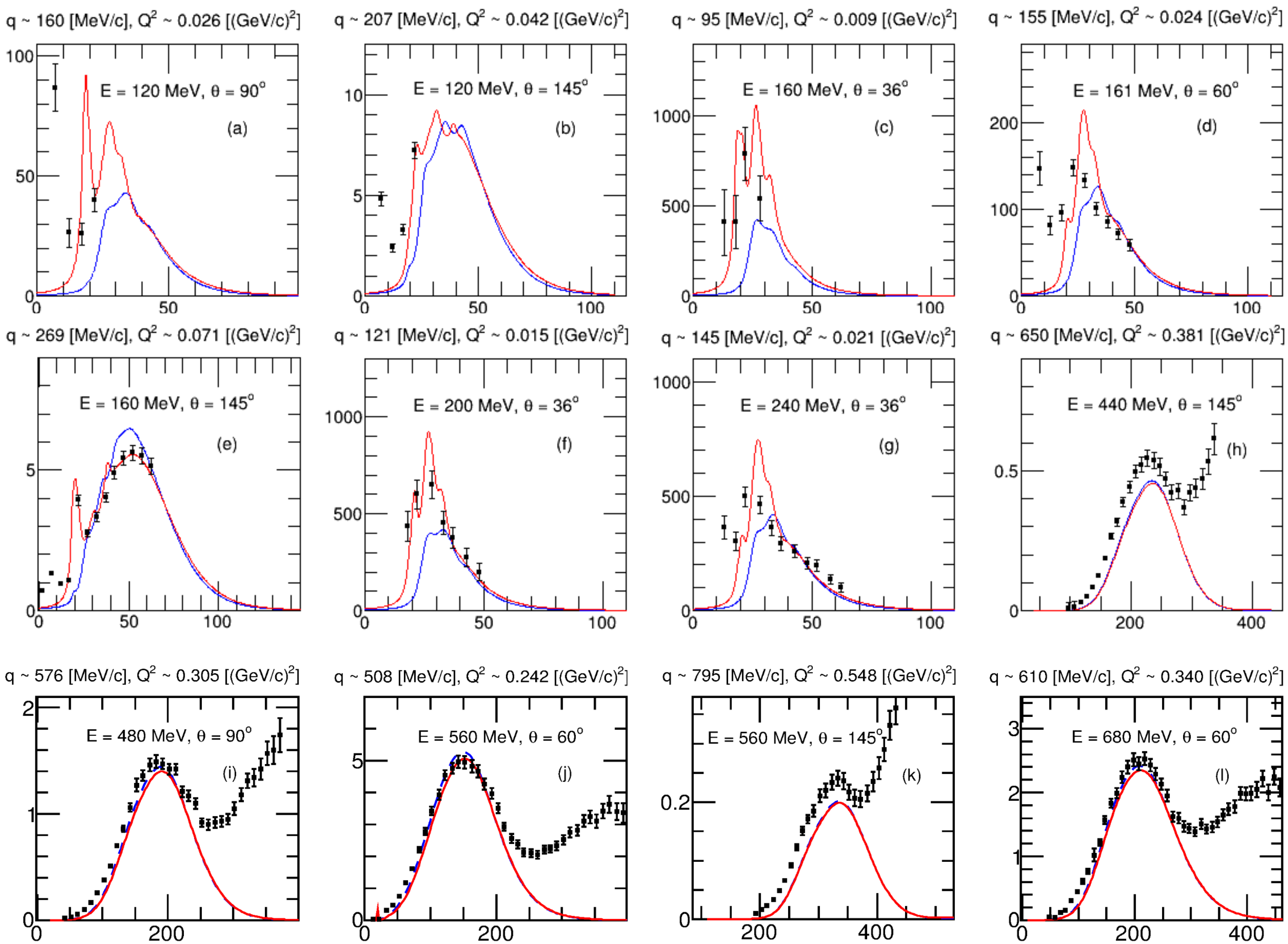

HF (blue) vs CRPA (red)

[V. Pandey PhD Thesis; PRC 92, 024606 (2015)]

Low-energy contributions in flux-folded XS

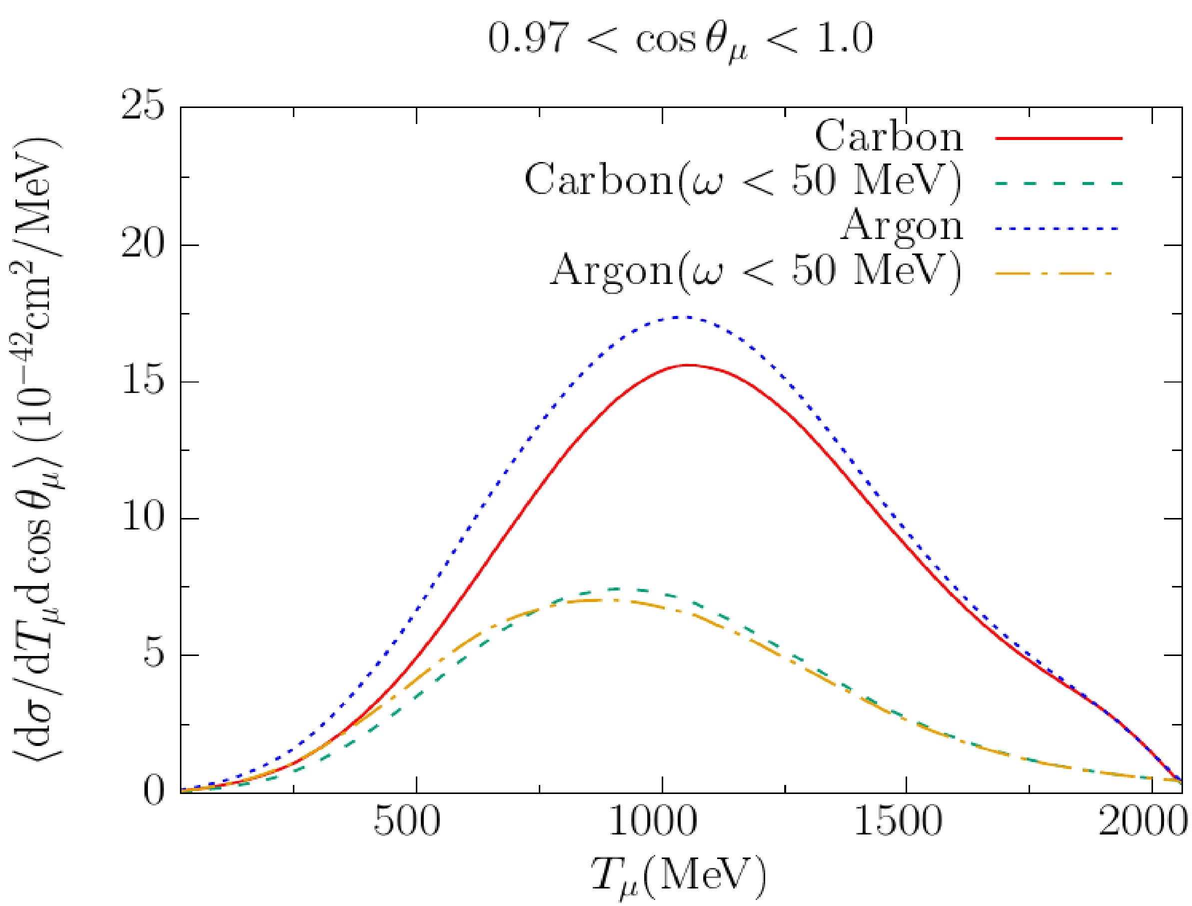

MicroBooNE flux-folded cross section.

Two-nucleon knockout processes

In our approach, two mechanisms give rise to the emission of two nucleons:

Short-range correlations

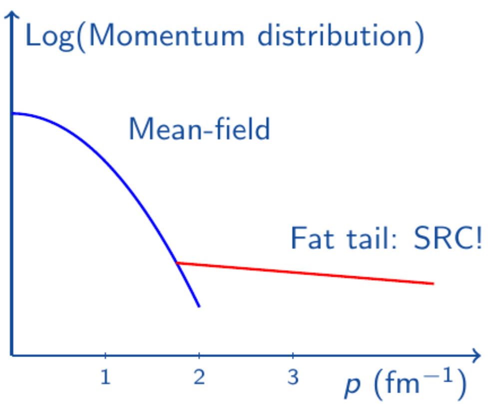

Meson-exchange currents

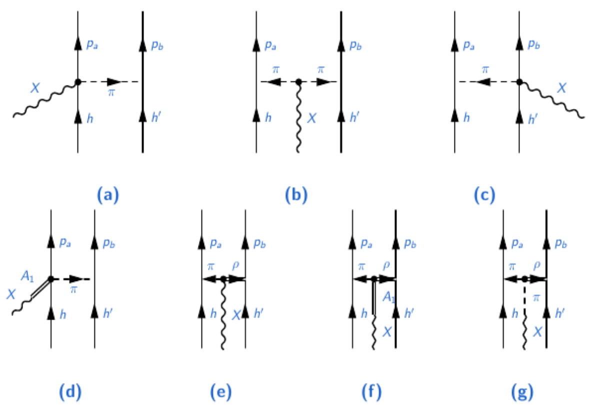

T. Van Cuyck's PhD Thesis

The same **mean-field** model is used to describe the **bound and scattered nucleons**:

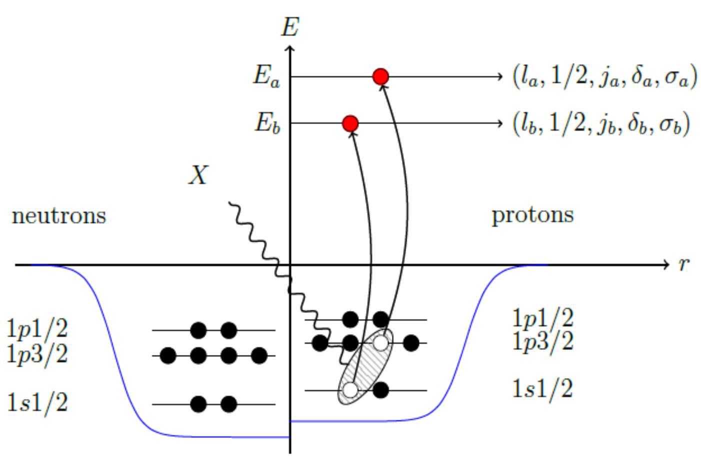

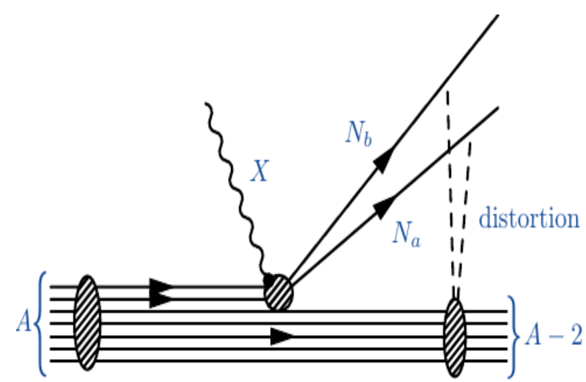

Short range correlations

$$|\Psi\rangle = \frac{1}{\sqrt{\mathcal{N}}}\widehat{\mathcal{G}}|\Phi\rangle \qquad \text{with} \qquad \widehat{\mathcal{G}} \approx \widehat{\mathcal{S}}\left(\prod_{i<j}^{A}\left[1+\widehat{l}(i,j)\right]\right)$$

$$\widehat{l}(i,j) = -\,g_c(r_{ij}) + f_{\sigma\tau}(r_{ij})\,(\vec{\sigma}_i\cdot\vec{\sigma}_j)\,(\vec{\tau}_i\cdot\vec{\tau}_j)$$
$$+\,f_{t\tau}(r_{ij})\widehat{S}_{ij}\,(\vec{\tau}_i\cdot\vec{\tau}_j)\,,$$

The complexity induced by correlations is shifted from the wave functions to the operators

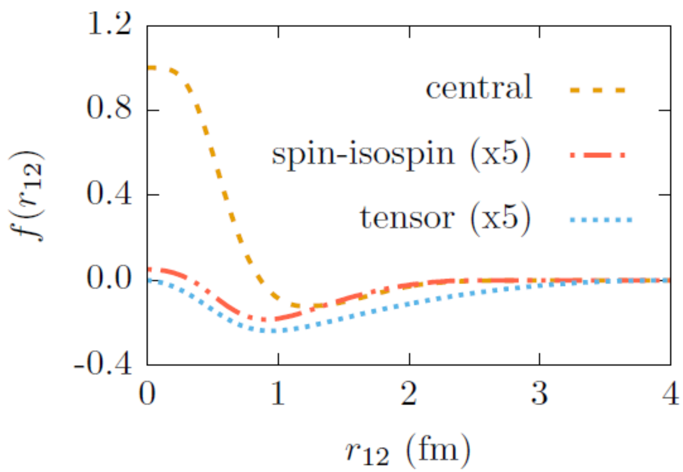

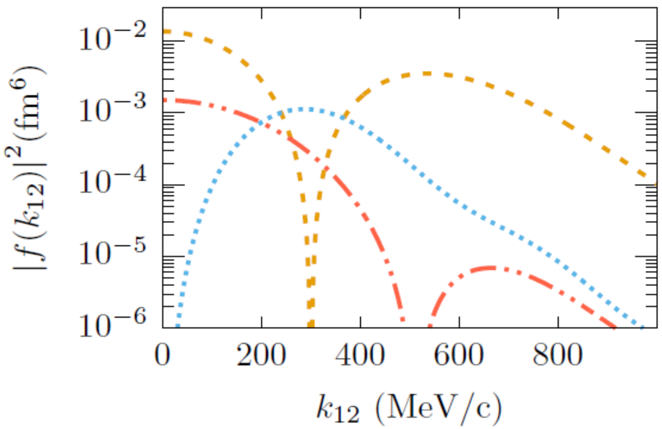

Short range correlations

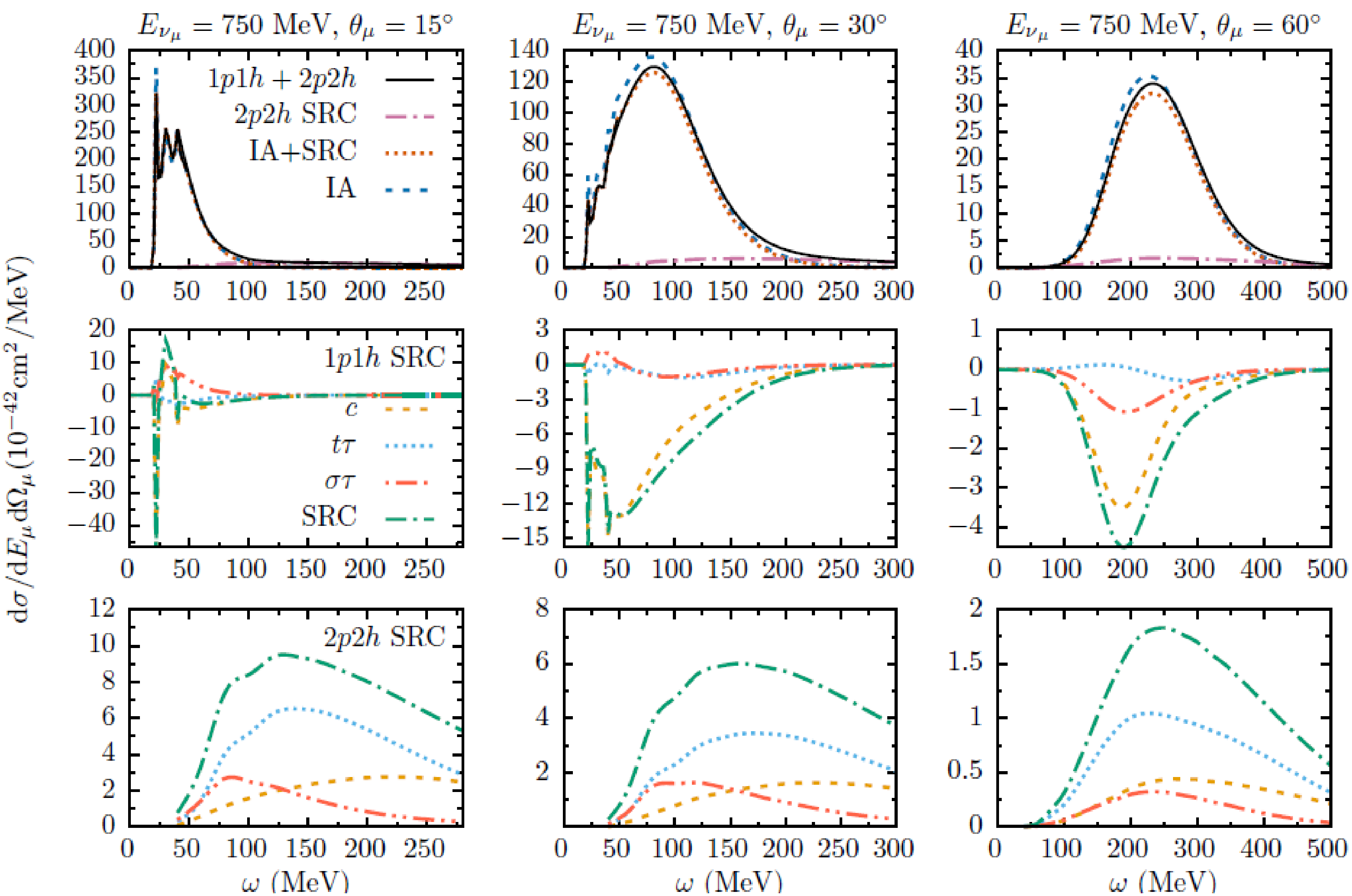

SRC affect the 1p1h and the 2p2h responses

Van Cuyck et al., Phys. Rev. C 94, 024611 (2016)

Meson-exchange currents

Van Cuyck et al., PRC 95, 054611 (2017)

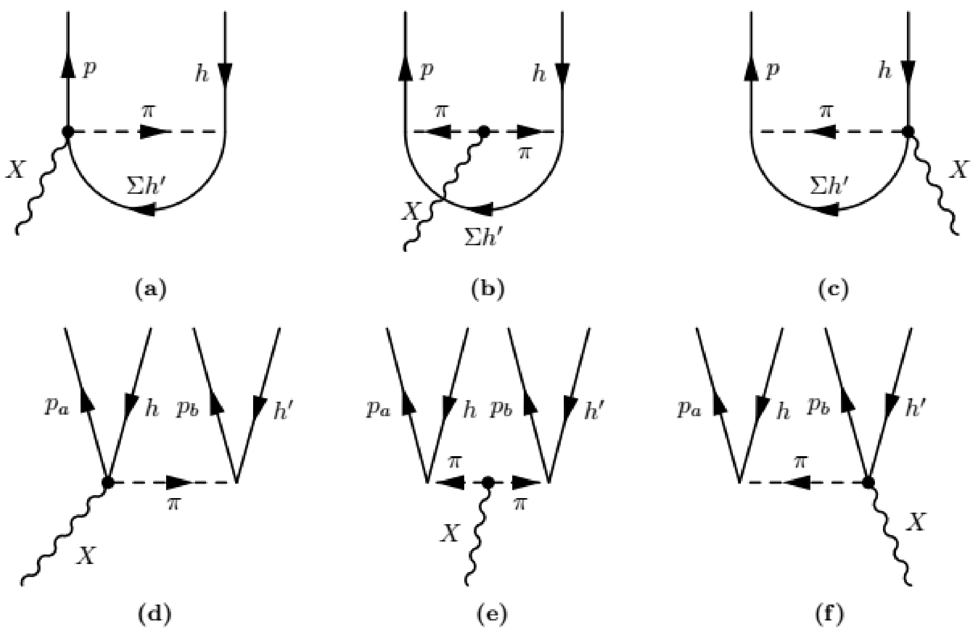

1p1h contributions (vector current)

2p2h contributions (vector current)

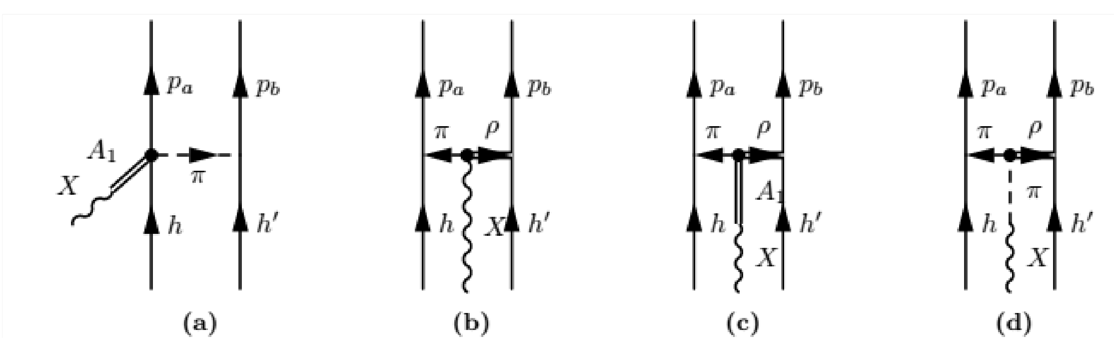

Axial current (1p1h and 2p2h)

Meson-exchange currents

Good agreement with other predictions [Amaro et al., NPA578, 365 (1994)]:

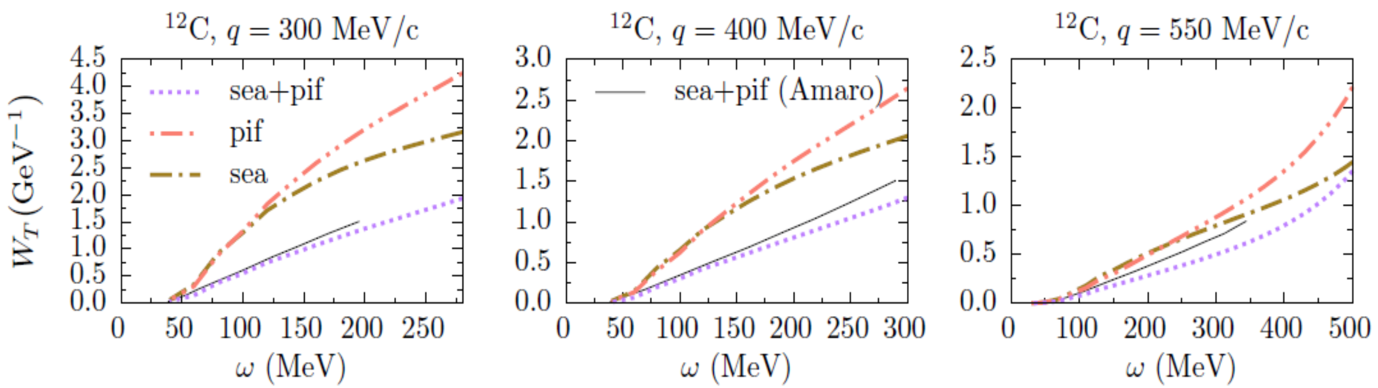

1p1h and 2p2h contributions to the longitudinal and transverse responses:

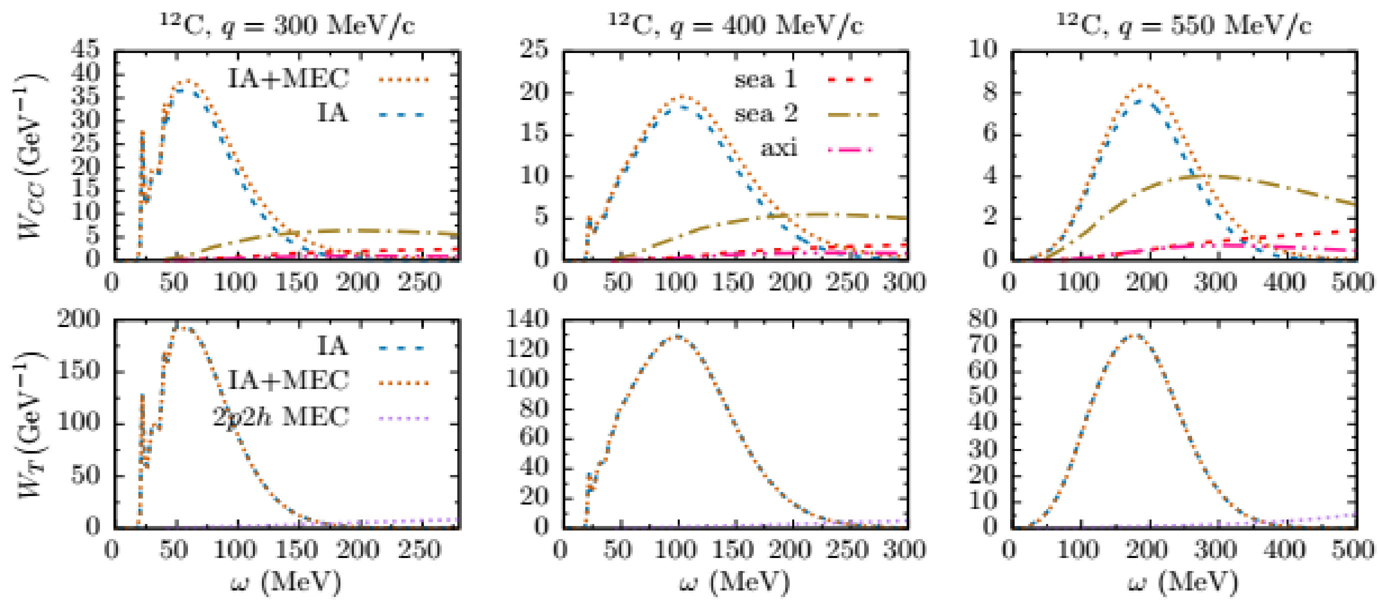

Meson-exchange currents

In spite of the complexity and ambiguities of the calculation, we find good agreement with other p

Exclusive, as well.

1p1h and 2

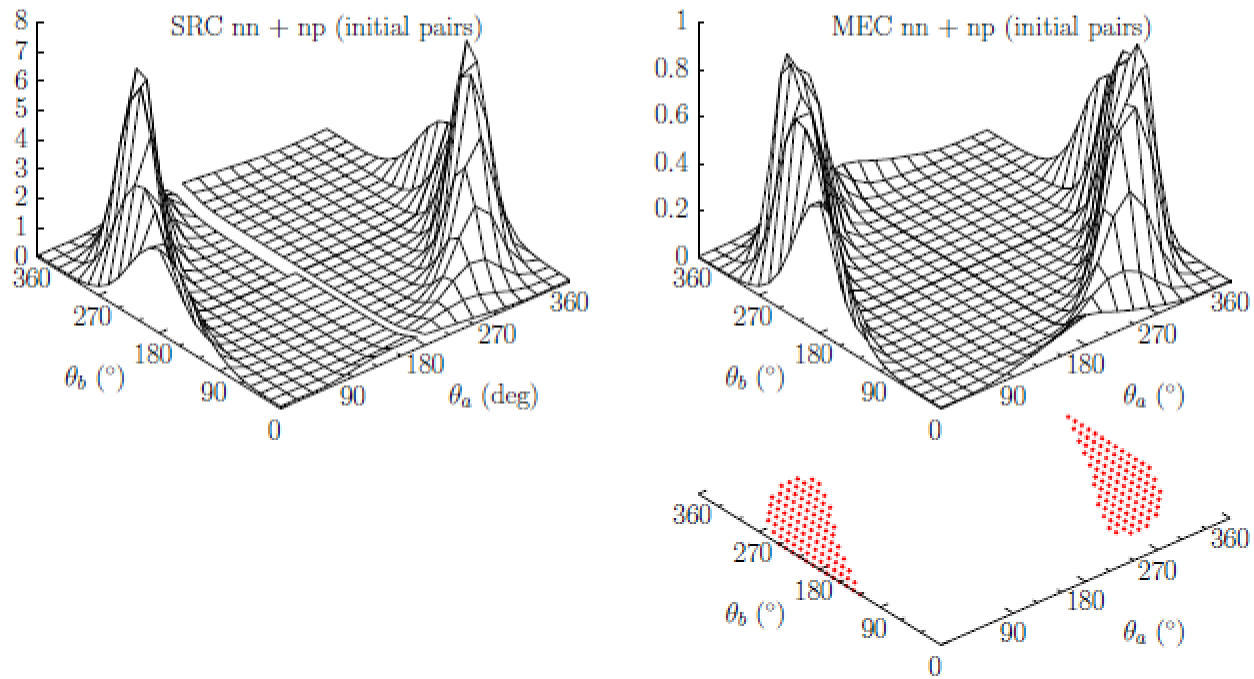

Figure 4.5: The ^{12}C$(\nu_\mu, \mu^- N_a N_b)$ cross section (N_a = p, N_b = p′, n) at ϵ_{ν_μ} = 750 MeV, ϵ_μ = 550 MeV, $\theta_\mu = 15°$ and $T_{\rm p}$ = 50 MeV for in-plane kinematics. Left with SRCs, right with MECs, the bottom plot shows the (θ_a, θ_b) regions with $P_{12} < 300$ MeV/c.

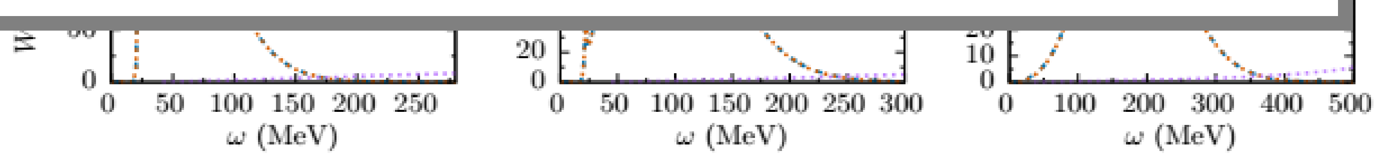

Flux folded xs: MiniBooNE & T2K

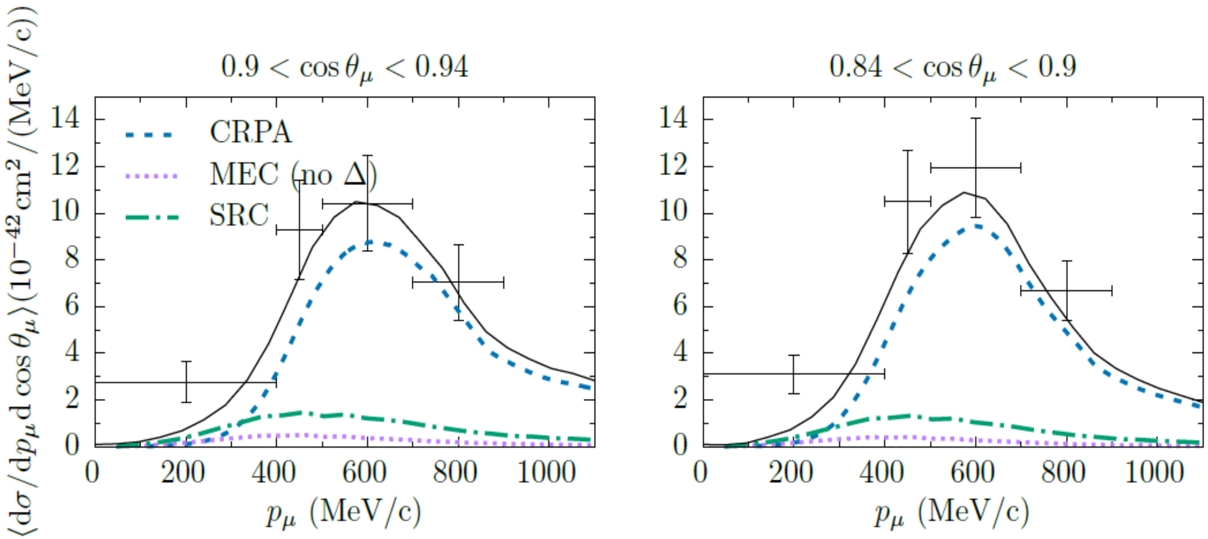

T2K

(inclusive: QE, 2p2h, pions, DIS)

MiniBooNE

(QE-like: QE+2p2h)

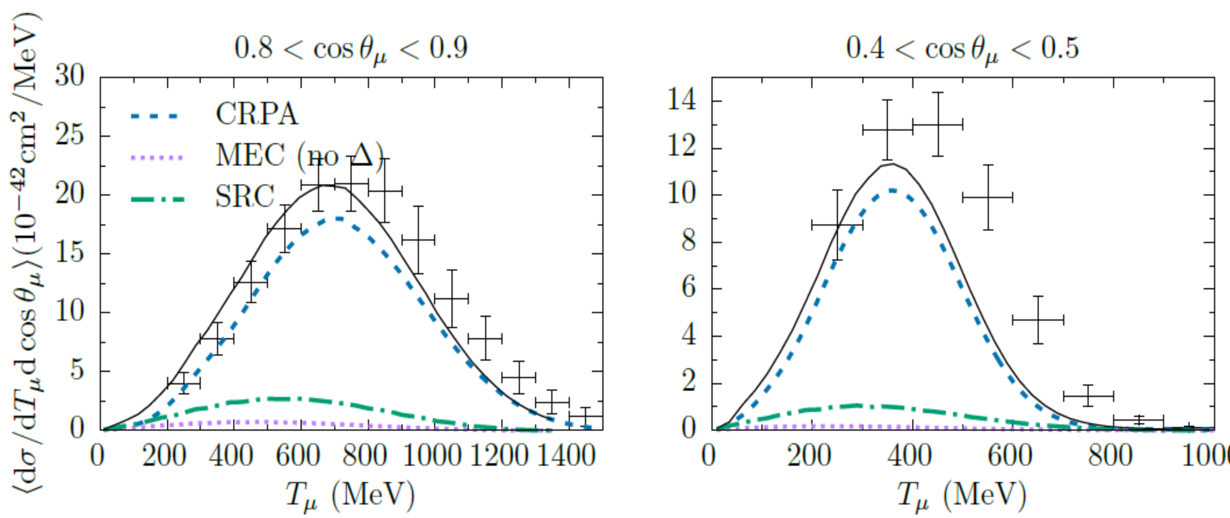

Single-Pion Production on the nucleon

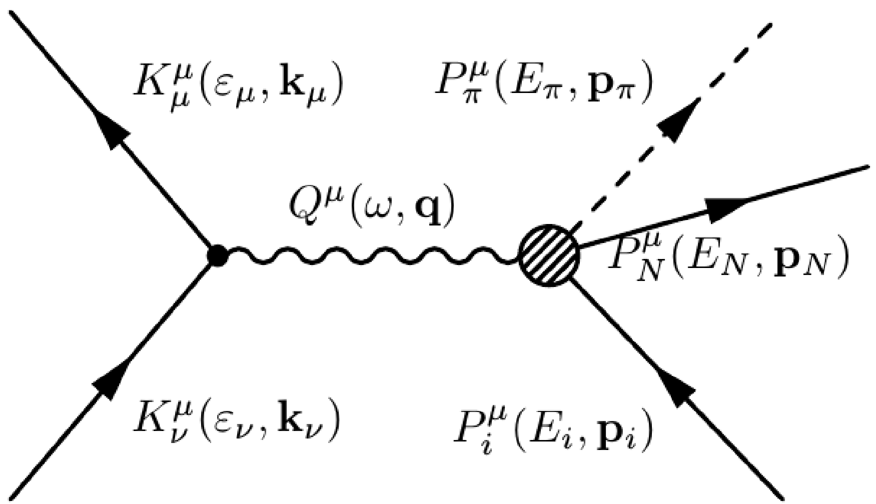

González-Jiménez et al., PRD 95, 113007 (2017)

Electroweak single-pion production

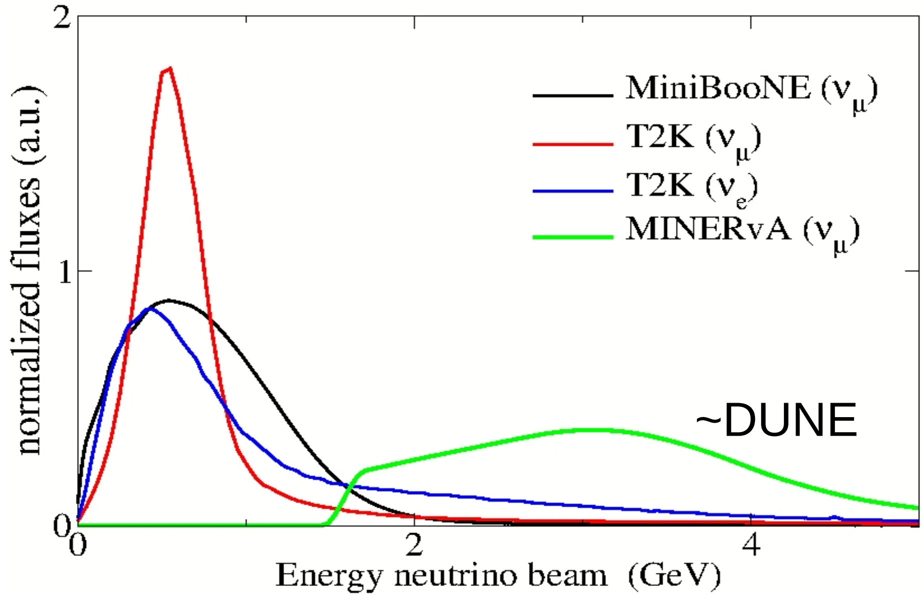

Pion production is more important for DUNE

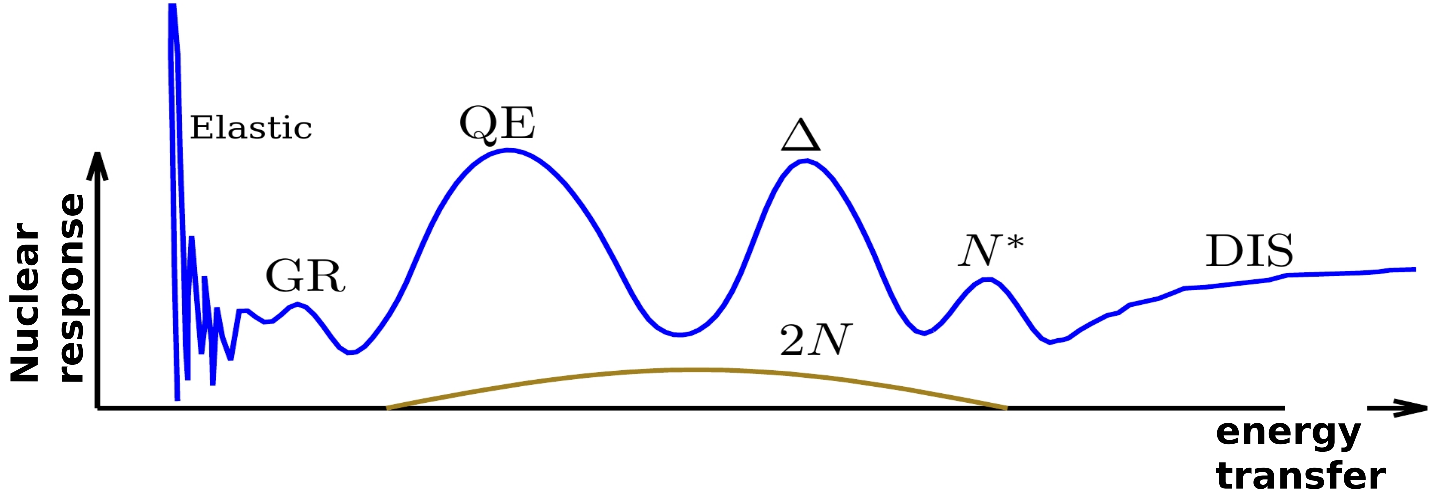

Low-energy model

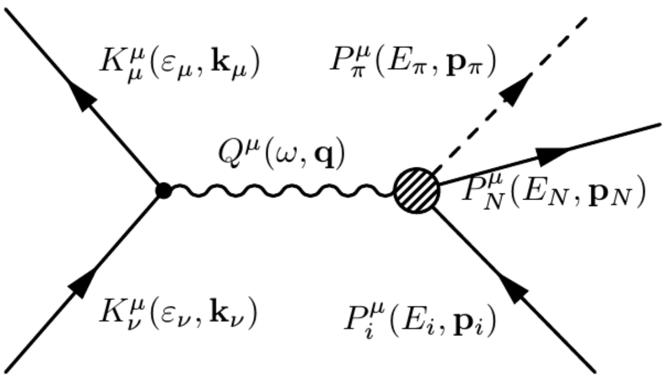

Low-energy model for pion-production on the nucleon:
ChPT background + resonances
Valencia model (PRD 76 (2007) 033005, PRD 87 (2013) 113009)

Resonances:
P33(1232), D13(1520), S11(1535), P11(1440)

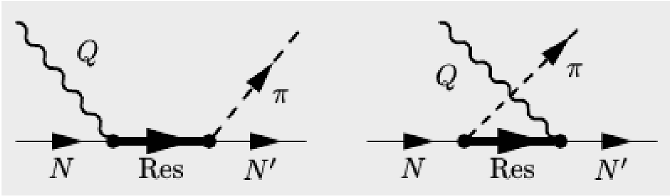

ChPT background:

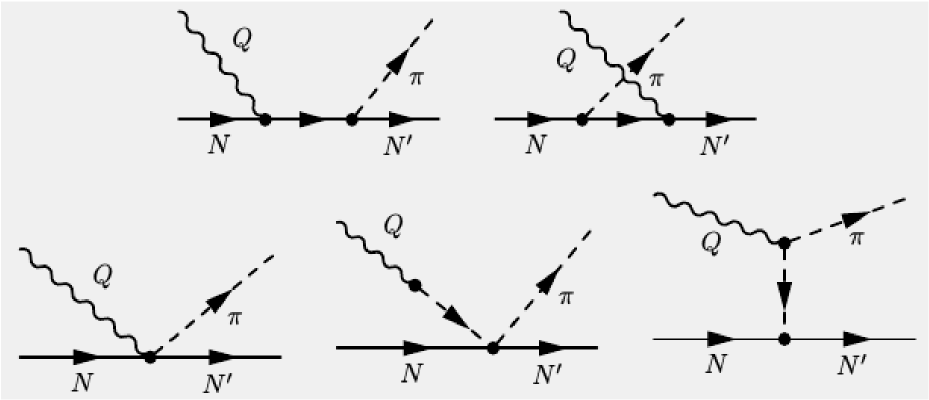

The Problem

Low-energy model
(resonances + ChPT bg)

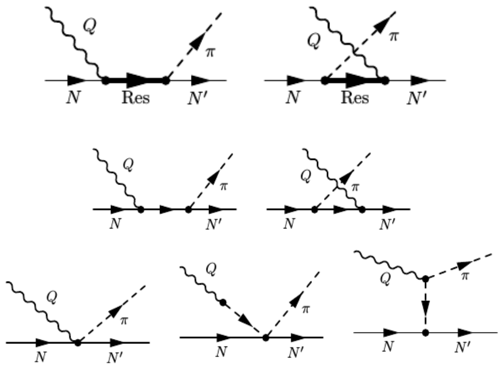

Unphysical predictions at large invariant masses.

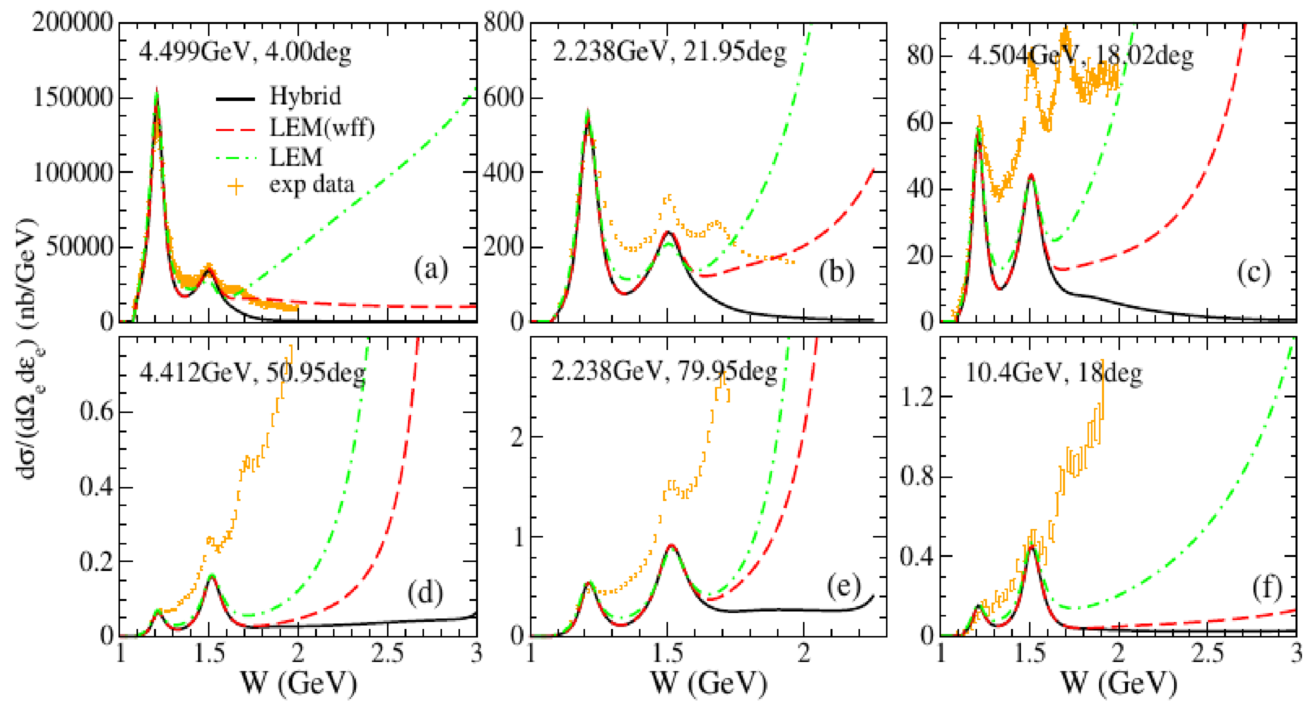

Figure: The model overshoots **inclusive electron-proton** scattering data.

The Problem

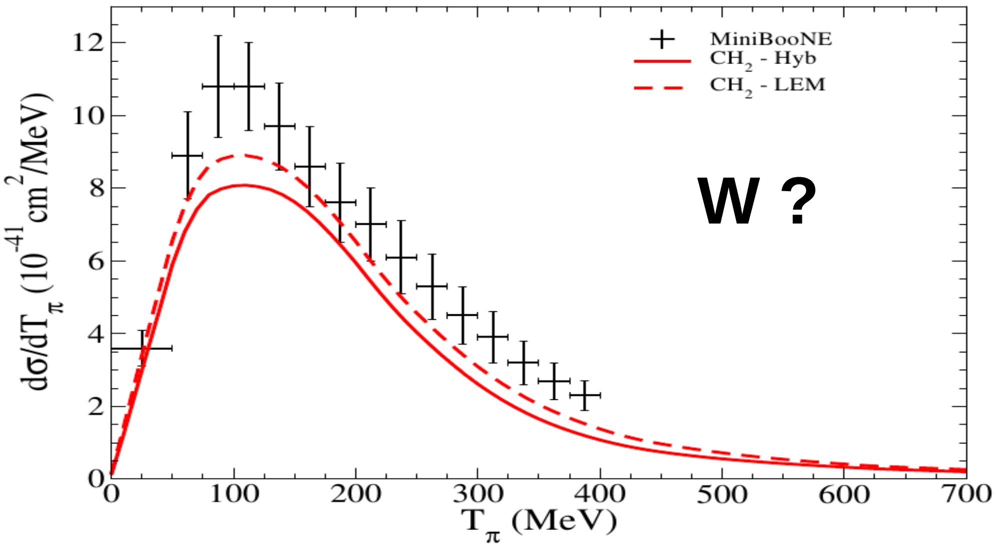

W values? We don't know...
+ Fermi motion
+ Flux-folding

Therefore, we need reliable predictions in:

+ the **resonance region** W < 2 GeV,

+ the **high-energy** energy region W > 2 GeV

High-energy model

Regge approach for the vector amplitudes.

We use the approach of **Guidal, Laget, and Vanderhaeghen** [NPA627, 645 (1997)], originally developed for pion photoproduction ($Q^2 = 0$):

1) Feynman **meson-exchange diagrams** are reggeized.

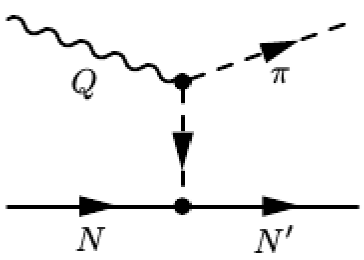

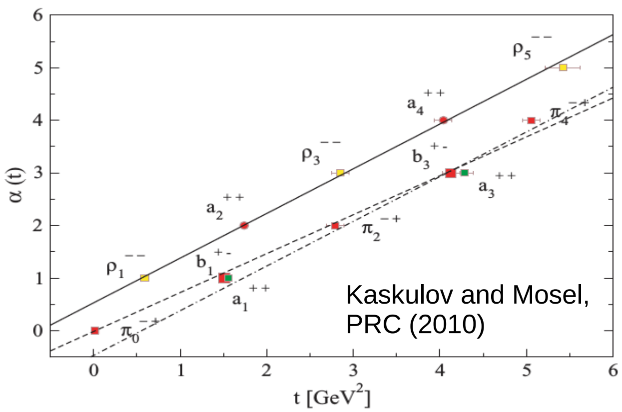

$$\frac{1}{t - m_\pi^2}$$

The pion propagator is replace by the Regge trajectory of the pion family

$$\mathcal{P}_\pi(t,s) = -\alpha'_\pi \varphi_\pi(t) \Gamma[-\alpha_\pi(t)](\alpha'_\pi s)^{\alpha_\pi(t)}$$

High-energy model

Regge approach for the vector amplitudes.

We use the approach of **Guidal, Laget, and Vanderhaeghen** [NPA627, 645 (1997)], originally developed for pion photoproduction ($Q^2 = 0$):

1) Feynman **meson-exchange diagrams** are reggeized.

2) s-channel, u-channel, and contact term diagrams are included to keep **Conservation of Vector Current**.

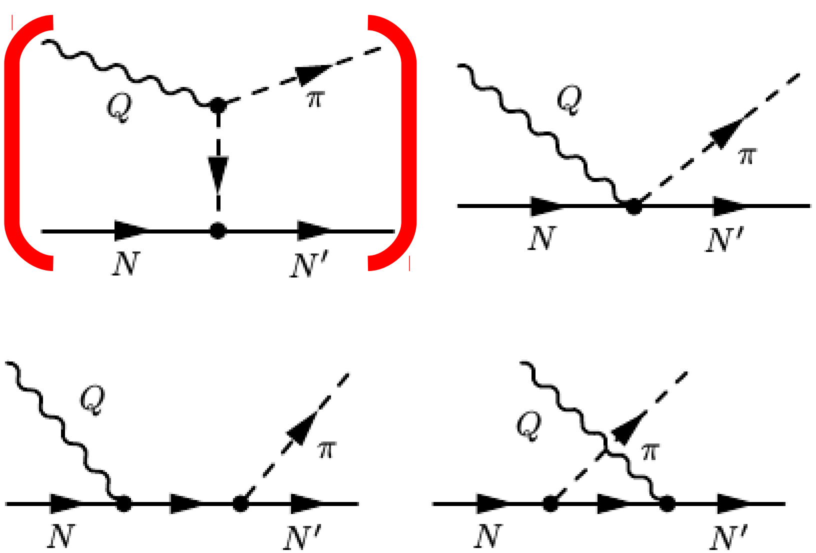

$$\frac{1}{t - m_\pi^2}$$

The pion propagator is replace by the Regge trajectory of the pion family

$$\mathcal{P}_\pi(t,s) = -\alpha'_\pi \varphi_\pi(t)\Gamma[-\alpha_\pi(t)](\alpha'_\pi s)^{\alpha_\pi(t)}$$

High-energy model: results (EM current)

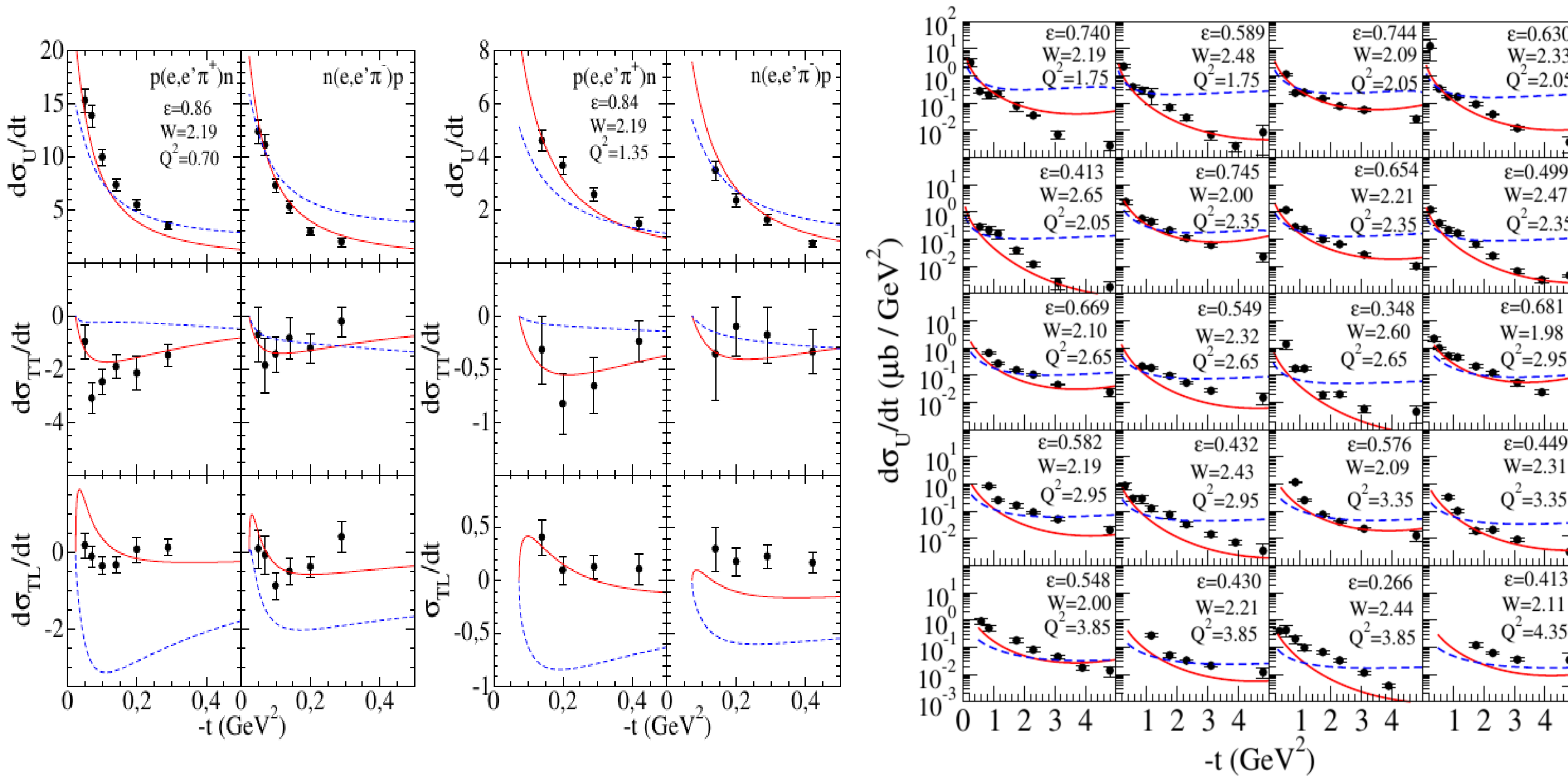

Figure: High-energy model (red lines), low-energy model (blue lines) and **electron-induced single-pion production** data.

High-energy model

Regge approach for the axial amplitudes.

We need meson exchange diagrams to apply the reggeization procedure of the current.

Effective rho-exchange diagrams. This allows us to consider the rho-exchange as the main Regge trajectory in the axial current.

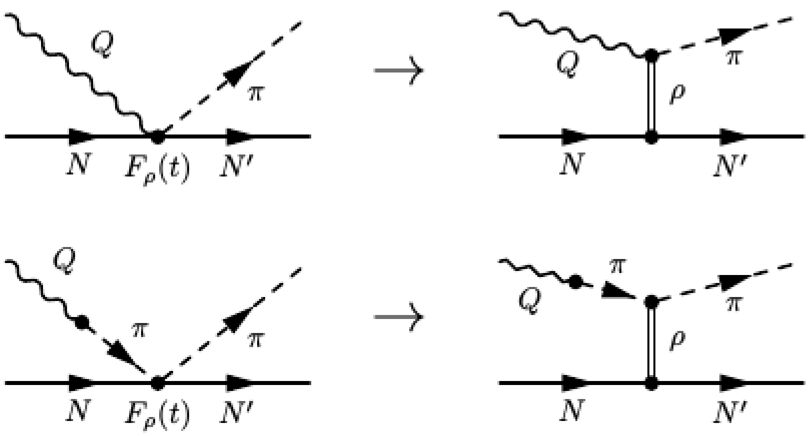

$$\mathcal{O}^{\mu}_{CT\rho} = i\mathcal{I}\frac{m_\rho^2}{m_\rho^2 - t} F_{A\rho\pi}(Q^2)\frac{1}{\sqrt{2}f_\pi} \times \left(\gamma^\mu + i\frac{\kappa_\rho}{2M}\sigma^{\mu\nu}K_{t,\nu}\right) .$$

We consider $\kappa_\rho = 0$ so that the low-energy model amplitude is recovered.

The propagator of the rho is replaced by the Regge trajectory of the **rho family**:

$$\mathcal{P}_\rho(t,s) = -\alpha'_\rho \varphi_\rho(t)\Gamma[1-\alpha_\rho(t)](\alpha'_\rho s)^{\alpha_\rho(t)-1}$$

High-energy model

Regge approach for the axial amplitudes.

We need meson exchange diagrams to apply the reggeization procedure of the current.

Effective rho-exchange diagrams. This allows us to consider the rho-exchange as the main Regge trajectory in the axial current.

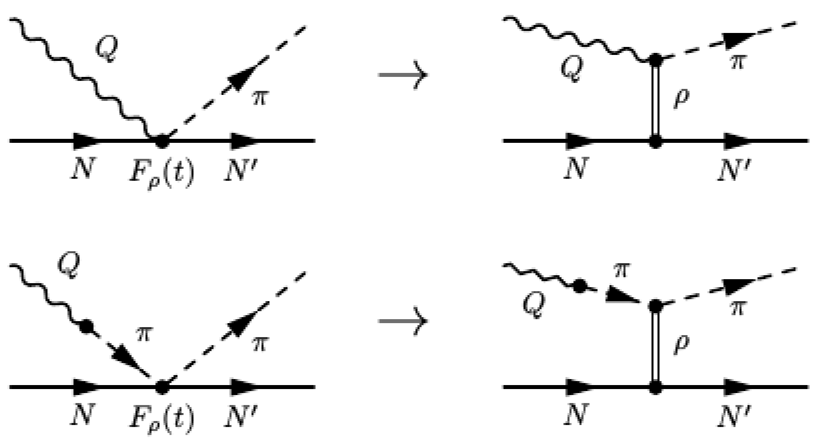

$$\mathcal{O}^{\mu}_{CT\rho} = i\mathcal{I}\,\frac{m_\rho^2}{m_\rho^2 - t} F_{A\rho\pi}(Q^2)\frac{1}{\sqrt{2}f_\pi} \times \left(\gamma^\mu + i\frac{\kappa_\rho}{2M}\sigma^{\mu\nu}K_{t,\nu}\right) .$$

We consider $\kappa_\rho = 0$ so that the low-energy model amplitude is recovered.

\+ 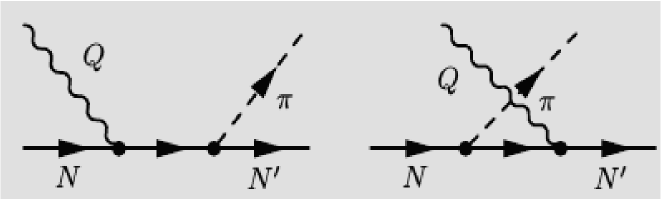

?

High-energy model

“Reggeizing” the ChPT background:

$$\mathcal{O}^{\mu}_{ReChi,V} = \mathcal{O}^{\mu}_{ChPT,V}\,\underbrace{\mathcal{P}_{\pi}(t,s)(t-m_{\pi}^{2})}$$

high-energy model: ReChi (from Reggeized ChPT background)

low-energy model (only the ChPT background)

The pion propagator is replaced by the **Regge propagator** of the pion trajectory

$$\mathcal{O}^{\mu}_{ReChi,A} = \mathcal{O}^{\mu}_{ChPT,A}\,\mathcal{P}_{\rho}(t,s)(t-m_{\rho}^{2})$$

Hybrid model: results

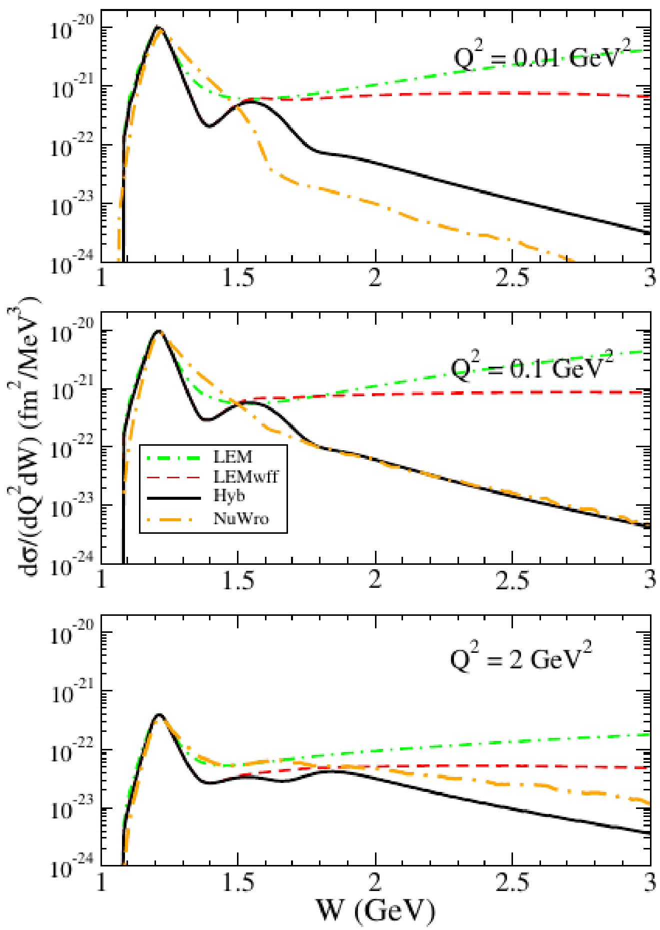

FIG. 21. (Color online) Different model predictions for the differential cross section $d\sigma/(dQ^2dW)$, for the channel $p(\nu_\mu, \mu^-\pi^+)p$. The incoming neutrino energy is fixed to $E_\nu = 10$ GeV.

Hybrid model: results

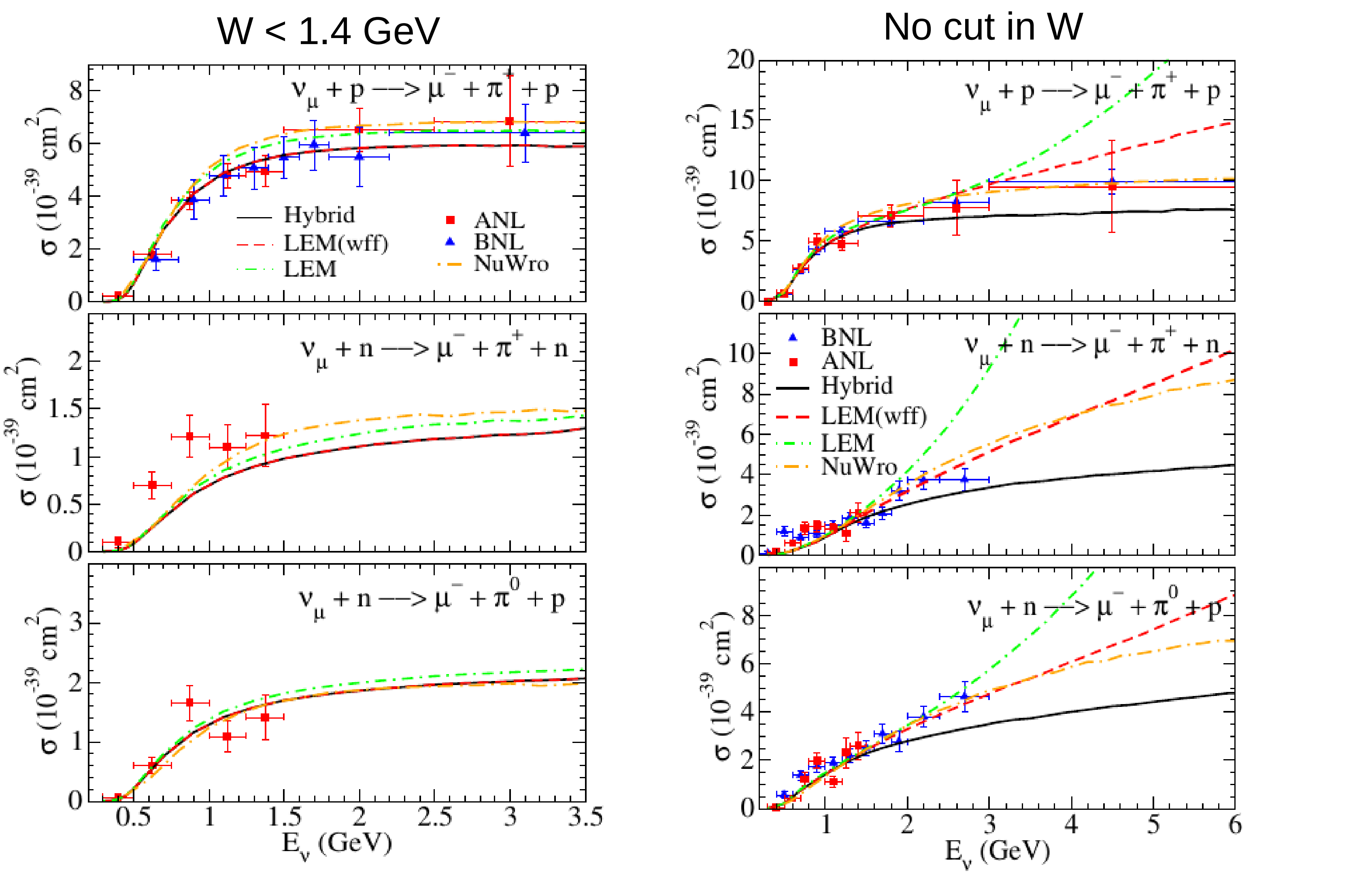

Electroweak one-pion production on nuclei

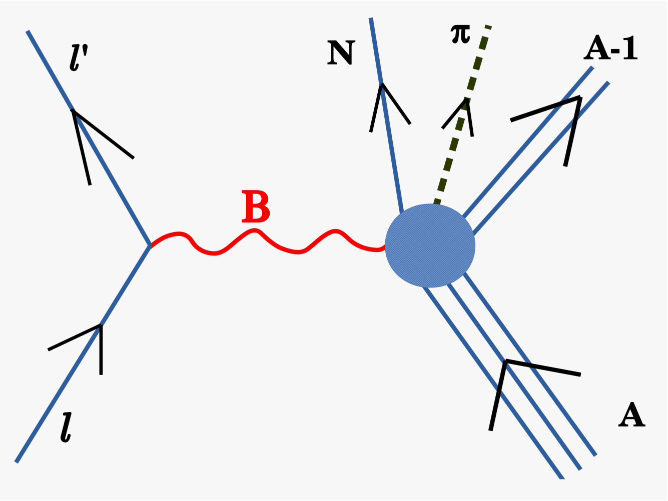

Relativistic mean field model

Relativistic Impulse Approximation

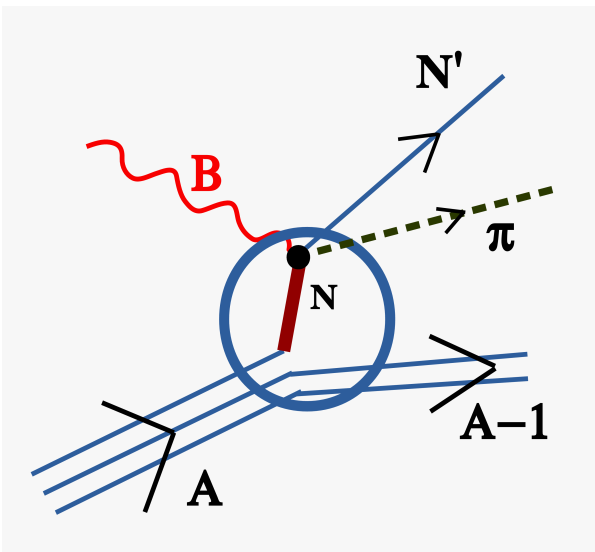

Plane waves (for the moment...)

$$J^{\mu}_{had} = \sum_i^A \int \mathrm{d}\mathbf{r}\, \overline{\Psi}_F(\mathbf{r})\, \phi^*(\mathbf{r}) \hat{\mathcal{O}}^{\mu}_{one\text{-}body}(\mathbf{r})\, \Psi_B(\mathbf{r})\, e^{i\mathbf{q}\cdot\mathbf{r}}$$

not yet

?

Relativistic mean-field wave functions

$$\frac{\mathrm{d}^8\sigma}{\mathrm{d}\varepsilon_f \mathrm{d}\Omega_f \mathrm{d}E_\pi \mathrm{d}\Omega_\pi \mathrm{d}\Omega_N} = \frac{m_i m_f}{(2\pi)^8} \frac{M_N\, p_N\, k_\pi}{E_N\, f_{rec}} \frac{k_f}{\varepsilon_i} \overline{\sum_{fi}} |\mathcal{M}_{fi}|^2$$

8-fold differential cross section: Computationally very demanding

MiniBooNE neutrino CC 1pion+.

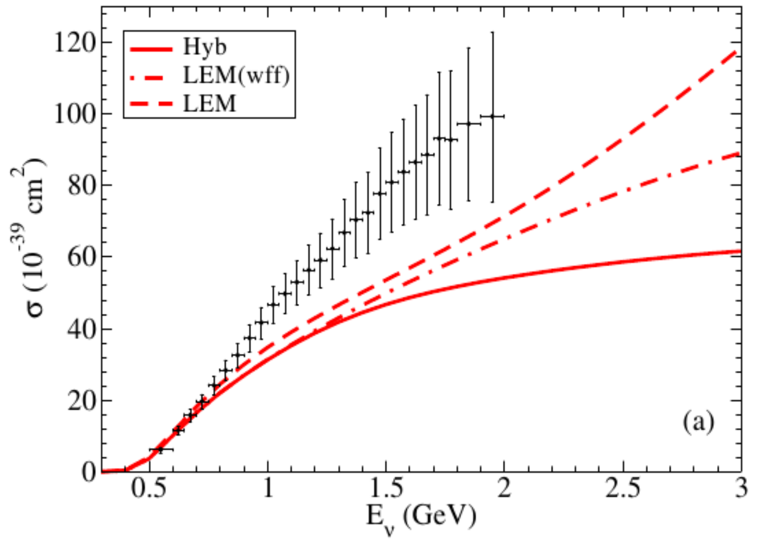

MINERvA antineutrino CC 1pion0.

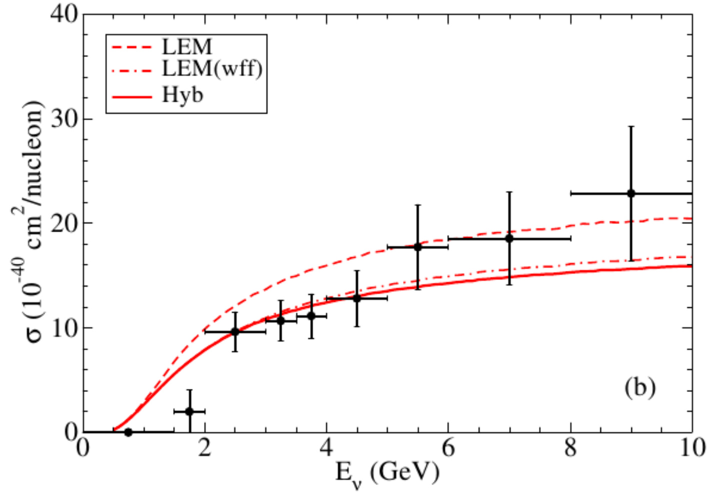

MiniBooNE neutrino CC 1pion+.

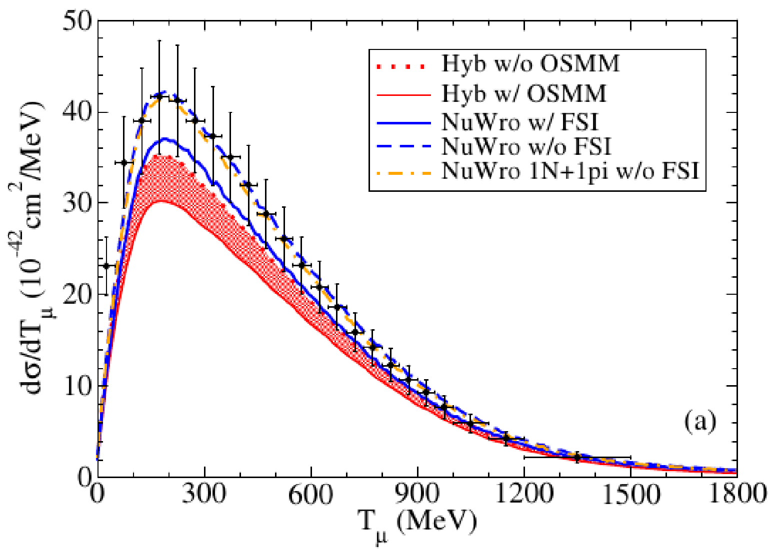

MINERvA antineutrino CC 1pion0.

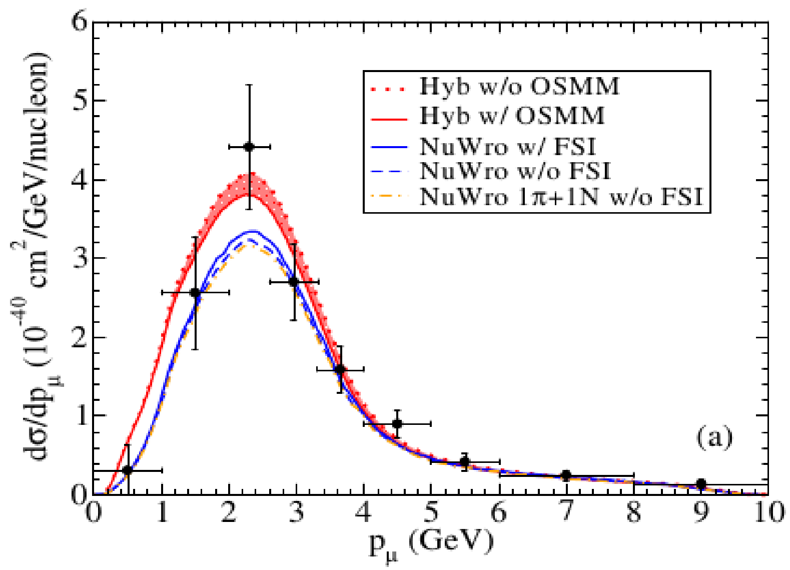

Conclusions

- ✔ **QE scattering: Mean-field wave functions** in both bound and scattered nucleon are important: long tails in inclusive cross sections, redistribution of the strength, position of the peak.

- ✔ **2p2h** is induced by two mechanisms, **SRC and MEC**. Preferably, mean-field wave functions.

- ✔ **Single-pion production**: Low-energy models should not be used in high-W regions. We propose to combine the low-energy model with a Regge-based approach: **Hybrid model**.

Future: Lot of work to do...

The end...

Thanks for your attention

Backup slides

Long-range correlations: CRPA model

- Regularization of the residual interaction :

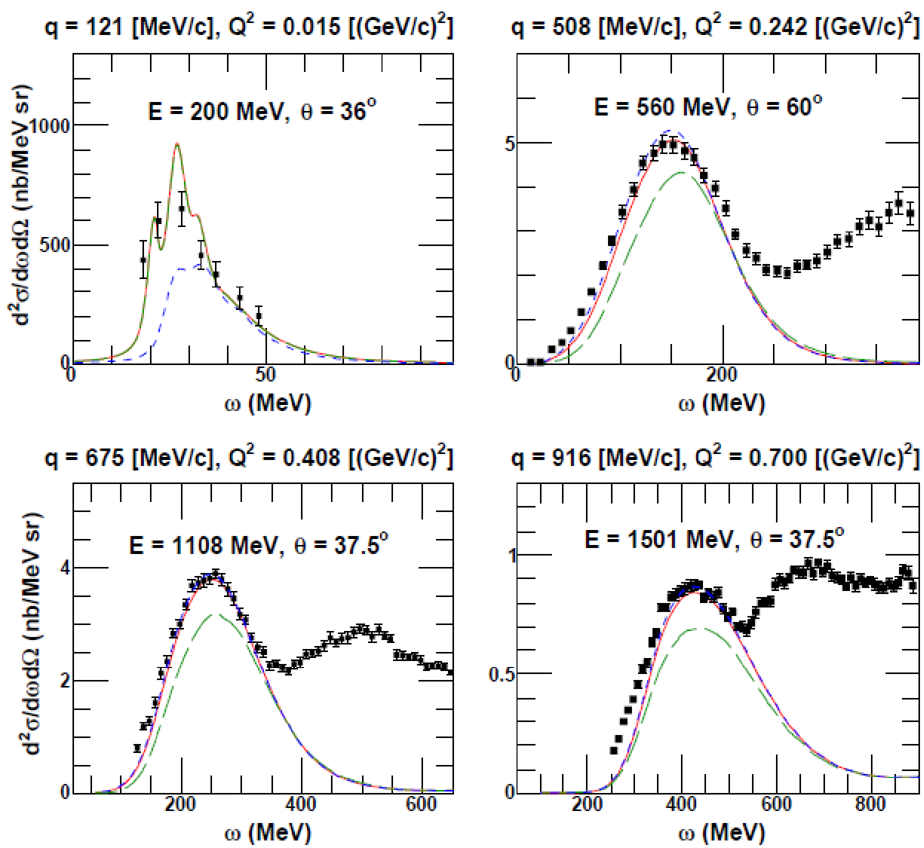

$$V(Q^2) \rightarrow V(Q^2=0)\,\frac{1}{(1+\frac{Q^2}{\Lambda^2})^2}$$

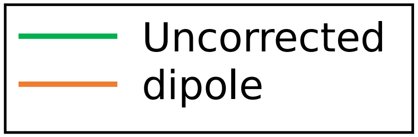

Relativizing the HF/CRPA predictions

Relativistic corrections at higher energies (J. Jeschonnek and T. Donnelly, PRC57, 2438 (1998)):

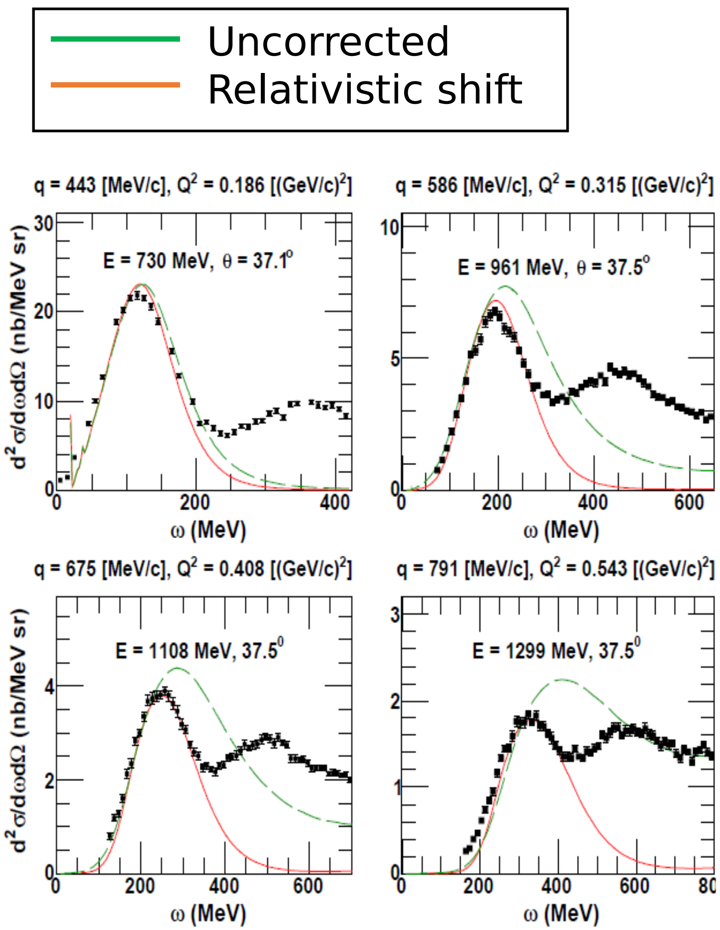

Shift :

$$\lambda \rightarrow \lambda(\lambda + 1) \qquad \lambda = \omega/2M_N$$

- The outgoing nucleon obtains the correct relativistic momentum
- Shifts the QE peak to the right relativistic position

Boost :

$$R^{\rm V}_{\rm CC}(q,\omega) \rightarrow \frac{q^2}{q^2-\omega^2} R^{\rm V}_{\rm CC}(q,\omega)\,,$$

$$R^{\rm A}_{\rm LL}(q,\omega) \rightarrow \left(1+\frac{q^2-\omega^2}{4m^2}\right) R^{\rm A}_{\rm LL}(q,\omega)\,,$$

$$R^{\rm V}_{\rm T}(q,\omega) \rightarrow \frac{q^2-\omega^2}{q^2} R^{\rm V}_{\rm T}(q,\omega)\,,$$

$$R^{\rm A}_{\rm T}(q,\omega) \rightarrow \left(1+\frac{q^2-\omega^2}{4m^2}\right) R^{\rm A}_{\rm T}(q,\omega)\,,$$

$$R^{\rm VA}_{\rm T'}(q,\omega) \rightarrow \sqrt{\frac{q^2-\omega^2}{q^2}}\sqrt{1+\frac{q^2-\omega^2}{4m^2}}\, R^{\rm VA}_{\rm T'}(q,\omega)\,.$$

Folding procedure

V. Pandey's PhD Thesis

- A limitation of RPA formalism at lower energies:
  - → energy position of the giant resonances is generally well predicted
  - → width is underestimated
  - → height is overestimated

Folding

$$R'(q,\omega') = \int_{-\infty}^{\infty} d\omega R(q,\omega) L(\omega,\omega')$$

$$L(\omega,\omega') = \frac{1}{2\pi}\left[\frac{\Gamma}{(\omega-\omega')^2+(\Gamma/2)^2}\right]$$

$\Gamma = 3$ MeV

CRPA: Without Folding, CRPA: With Folding

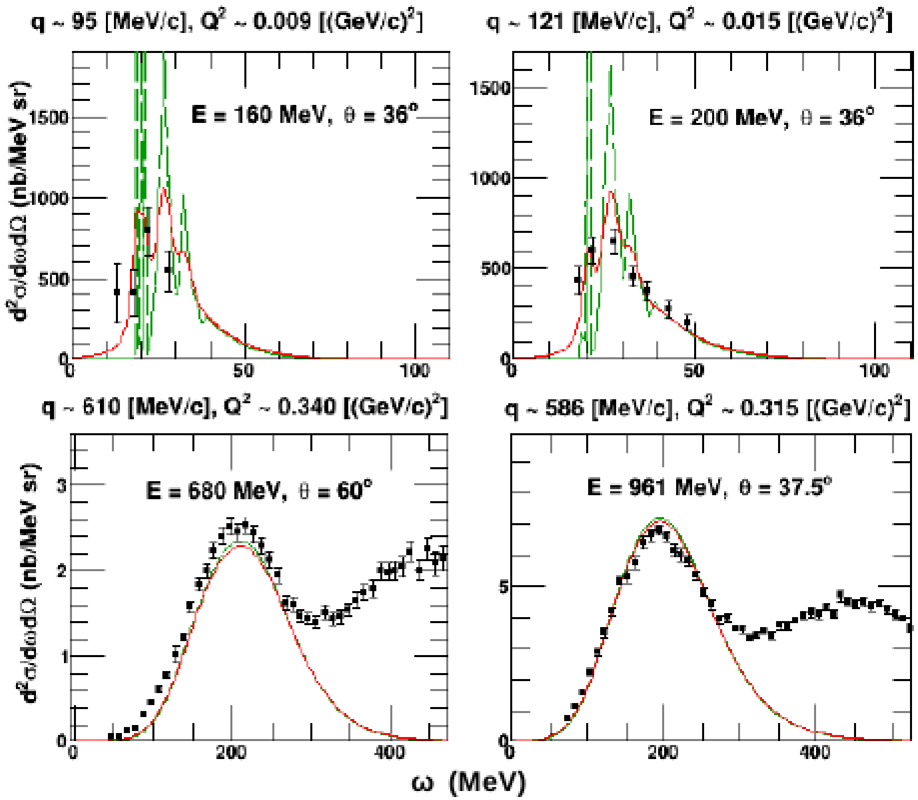

Relativistic mean-field model

RMF model provides a microscopic description of the ground state of finite nuclei which is consistent with Quantum Mechanic, Special Relativity and symmetries of strong interaction.

Extension of the original σ–ω Walecka model (Ann. Phys.83,491 (1974)).

The starting point is a Lorentz covariant Lagrangian density

$$
\begin{aligned}
\mathcal{L} &= \overline{\Psi}\left(i\gamma_\mu\partial^\mu - M\right)\Psi + \frac{1}{2}\left(\partial_\mu\sigma\partial^\mu\sigma - m_\sigma^2\sigma^2\right) - U(\sigma) \\
&- \frac{1}{4}\Omega_{\mu\nu}\Omega^{\mu\nu} + \frac{1}{2}m_\omega^2\omega_\mu\omega^\mu - \frac{1}{4}\mathbf{R}_{\mu\nu}\mathbf{R}^{\mu\nu} + \frac{1}{2}m_\rho^2\boldsymbol{\rho}_\mu\boldsymbol{\rho}^\mu - \frac{1}{4}F_{\mu\nu}F^{\mu\nu} \\
&- g_\sigma\overline{\Psi}\sigma\Psi - g_\omega\overline{\Psi}\gamma_\mu\omega^\mu\Psi - g_\rho\overline{\Psi}\gamma_\mu\boldsymbol{\tau}\boldsymbol{\rho}^\mu\Psi - g_e\frac{1+\tau_3}{2}\overline{\Psi}\gamma_\mu A^\mu\Psi\,.
\end{aligned}
$$

where

$$
\begin{aligned}
\Omega^{\mu\nu} &= \partial^\mu\omega^\nu - \partial^\nu\omega^\mu\,, \\
\boldsymbol{R}^{\mu\nu} &= \partial^\mu\boldsymbol{\rho}^\nu - \partial^\nu\boldsymbol{\rho}^\mu\,, \\
F^{\mu\nu} &= \partial^\mu A^\nu - \partial^\nu A^\mu\,. \\
U(\sigma) &= \tfrac{1}{3}g_2\sigma^3 + \tfrac{1}{4}g_3\sigma^4
\end{aligned}
$$

Main approximations:

1) Mean-field approximation:

$\omega_\mu \rightarrow \langle\omega_\mu\rangle$ $\sigma \rightarrow \langle\sigma\rangle$ $\boldsymbol{\rho}_\mu \rightarrow \langle\boldsymbol{\rho}_\mu\rangle$

2) Static limit:

$\partial^0\omega_0 = \partial^0\boldsymbol{\rho}_0 = \partial^0\sigma = 0$ $\omega_\mu = \delta_{\mu 0}\omega_0\,, \quad \boldsymbol{\rho}_\mu = \delta_{\mu 0}\boldsymbol{\rho}_0$

3) Spherical symmetry for finite nuclei:

$\omega_0 = \omega_0(r)$ $\boldsymbol{\rho}_0 = \boldsymbol{\rho}_0(r)$ $\sigma = \sigma(r)$

Relativistic mean-field model

Dirac equation for nucleons (eq. of motion for the barionic fields):

$$[-i\boldsymbol{\alpha}\cdot\boldsymbol{\nabla} + V(r) + \beta(M + S(r)]\Psi_i(\boldsymbol{r}) = E_i\Psi_i(\boldsymbol{r})$$

where the scalar (S) and vector (V) potential are given by:

$$\begin{aligned} S(r) &= g_\sigma \sigma(r)\,, \\ V(r) &= g_\omega \omega^0(r) + g_\rho \tau_3 \rho_3^0(r) + e\frac{1+\tau_3}{2}A^0(r) \end{aligned}$$

Eqs. of motion for the mesons and the photon:

$$\begin{aligned} \left[-\nabla^2 + m_\sigma^2\right]\sigma(r) &= -g_\sigma \rho_s(r) - g_2\sigma^2(r) - g_3\sigma^3(r)\,, \\ \left[-\nabla^2 + m_\omega^2\right]\omega^0(r) &= -g_\omega \rho_B(r)\,, \\ \left[-\nabla^2 + m_\rho^2\right]\rho_3^0(r) &= -g_\rho \rho_\rho(r)\,, \\ -\nabla^2 A^0 &= e\rho_c\,, \end{aligned}$$

Current densities

$$\begin{aligned} \rho_s(r) &= \sum_i^A \overline{\Psi}_i(\boldsymbol{r})\Psi_i(\boldsymbol{r})\,, \\ \rho_B(r) &= \sum_i^A \Psi_i^\dagger(\boldsymbol{r})\Psi_i(\boldsymbol{r})\,, \\ \rho_\rho(r) &= \sum_i^A \Psi_i^\dagger(\boldsymbol{r})\tau_3\Psi_i(\boldsymbol{r}) \\ \rho_c(r) &= \sum_i^A \Psi_i^\dagger(\boldsymbol{r})\frac{1+\tau_3}{2}\Psi_i(\boldsymbol{r}) \end{aligned}$$

Solution of the couple equations for the fields in a self-consistent way.

Relativistic mean-field model

In general, the parameters are fit to reproduce some general properties of some closed shell spherical nuclei and nuclear matter.

Parameters for the NLSH model (fitted to the mean charge radius, binding energy and neutron radius of the ^{16}**O,** ^{40}**Ca,** ^{90}**Zr,** ^{116}**Sr,** ^{124}**Sn** and ^{208}**Pb.**

M_N	m_σ	m_ω	m_ρ	g_σ	g_ω	g_ρ	g_2	g_3
939.0	526.059	783.0	763.0	10.444	12.945	4.3830	-6.9099	-15.8337

6 free parameters

$$[-i\boldsymbol{\alpha}\cdot\boldsymbol{\nabla} + V(r) + \beta(M + S(r)]\Psi_i(\boldsymbol{r}) = E_i\Psi_i(\boldsymbol{r})$$

$$\Psi_k^{m_j}(\boldsymbol{r}) = \begin{pmatrix} g_k(r)\varphi_k^{m_j}(\Omega_r) \\ i f_k(r)\varphi_{-k}^{m_j}(\Omega_r) \end{pmatrix},$$

$$\varphi_k^{m_j}(\Omega_r) = \sum_{m_\ell s}\langle \ell m_\ell \tfrac{1}{2} s | j m_j\rangle Y_\ell^{m_\ell}(\Omega_r)\chi^s$$

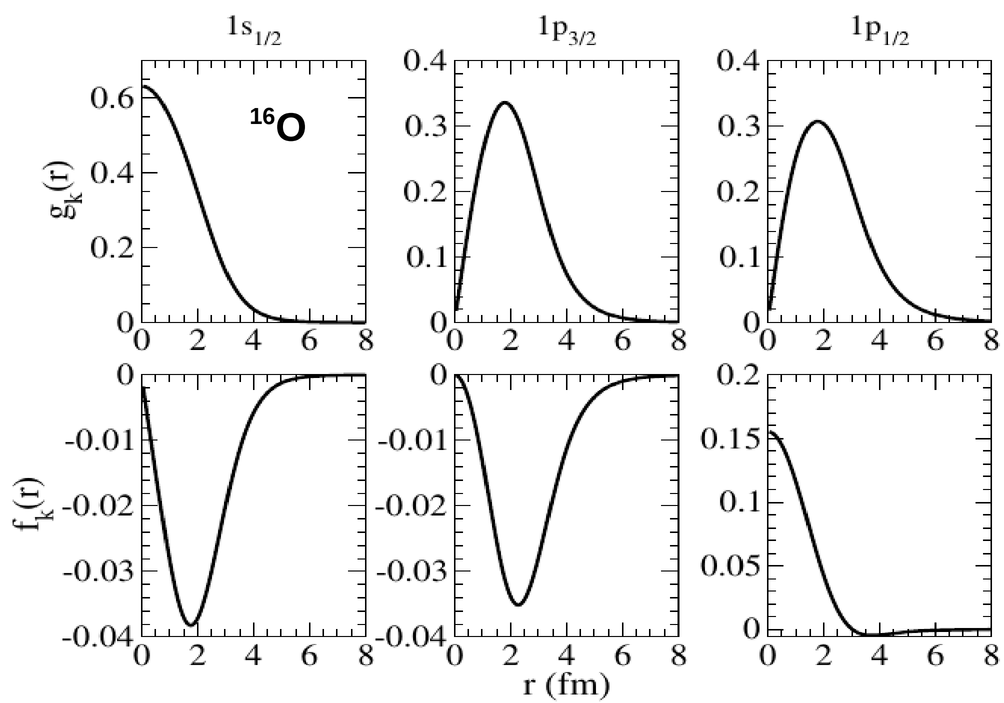

Back slides: isospin coefficients and resonances parameters

Channel	ΔP	$C\Delta P$	NP	CNP	Others
$p \to \pi^+ + p$	$\sqrt{3/2}$	$\sqrt{1/6}$	0	1	1
$n \to \pi^0 + p$	$-\sqrt{1/3}$	$\sqrt{1/3}$	$\sqrt{1/2}$	$-\sqrt{1/2}$	$-\sqrt{2}$
$n \to \pi^+ + n$	$\sqrt{1/6}$	$\sqrt{3/2}$	1	0	-1
$n \to \pi^- + n$	$\sqrt{3/2}$	$\sqrt{1/6}$	0	1	1
$p \to \pi^0 + n$	$\sqrt{1/3}$	$-\sqrt{1/3}$	$-\sqrt{1/2}$	$\sqrt{1/2}$	$\sqrt{2}$
$p \to \pi^- + p$	$\sqrt{1/6}$	$\sqrt{3/2}$	1	0	-1

Table: Isospin coefficients for the CC reaction.

Channel	ΔP	$C\Delta P$	NP	CNP	Others
$p \to \pi^0 + p$	$\sqrt{1/3}$	$\sqrt{1/3}$	$\sqrt{1/2}$	$\sqrt{1/2}$	0
$p \to \pi^+ + n$	$-\sqrt{1/6}$	$\sqrt{1/6}$	1	1	-1
$n \to \pi^- + p$	$\sqrt{1/6}$	$-\sqrt{1/6}$	1	1	1
$n \to \pi^0 + n$	$\sqrt{1/3}$	$\sqrt{1/3}$	$-\sqrt{1/2}$	$-\sqrt{1/2}$	0

Table: Isospin coefficients for the neutral current (EM and WNC) reactions.

	I	S	P	M_R	πN-br	$\Gamma^{exp}_{\text{width}}$	$f_{\pi NR}$
P_{33}	3/2	3/2	+	1232	100%	120	2.18
D_{13}	1/2	3/2	−	1515	60%	115	1.62
P_{11}	1/2	1/2	+	1430	65%	350	0.391
S_{11}	1/2	1/2	−	1535	45%	150	0.16

Table: quantum numbers and other parameters of the nucleon resonances.

Medium modifications of the Delta

Delta propagator:

$$S_{\Delta,\alpha\beta} = \frac{-(\not K_\Delta + M_\Delta)}{K_\Delta^2 - M_N^2 + iM_\Delta \Gamma_{\text{width}}} \left(g_{\alpha\beta} - \frac{1}{3}\gamma_\alpha\gamma_\beta - \frac{2}{3M_\Delta^2} K_{\Delta,\alpha} K_{\Delta,\beta} - \frac{2}{3M_\Delta}(\gamma_\alpha K_{\Delta,\beta} - K_{\Delta,\alpha}\gamma_\beta) \right)$$

with the energy dependent Delta width:

$$\Gamma_{\text{width}}(W) = \frac{1}{12\pi} \frac{(f_{\pi N\Delta})^2}{m_\pi^2 W} (p_{\pi,cm})^3 (M + E_{N,cm})$$

$$\Gamma_{\text{width}}^{\text{free}} \longrightarrow \Gamma_{\text{width}}^{\text{in-medium}} = \Gamma_{\text{Pauli}} - 2\Im(\Sigma_\Delta)\,, \qquad M_\Delta^{\text{free}} \longrightarrow M_\Delta^{\text{in-medium}} = M_\Delta^{\text{free}} + \Re(\Sigma_\Delta)\,.$$

- Γ_{Pauli}: some nucleons from Δ-decay are Pauli blocked (the Δ-decay width decreases).
- The parametrization of $\Im(\Sigma_\Delta)$ and $\Re(\Sigma_\Delta)$ is given in terms of the nuclear density ρ:

$$\begin{aligned} -\Im(\Sigma_\Delta) &= C_{QE}\,(\rho/\rho_0)^\alpha + C_{A2}\,(\rho/\rho_0)^\beta + C_{A3}\,(\rho/\rho_0)^\gamma \;, \\ \Re(\Sigma_\Delta) &= 40\text{ MeV}\,(\rho/\rho_0)\,. \end{aligned}$$

We modify the free $\Delta\pi N$-decay constant ($f_{\Delta\pi N}$) to take into account the E-dependent medium modification of the Δ width:

$$f_{\Delta\pi N}^{\text{in-medium}}(W) = f_{\Delta\pi N}\sqrt{\frac{\Gamma_{\text{Pauli}} + 2C_{QE}\,(\rho/\rho_0)^\alpha}{\Gamma_{\text{width}}^{\text{free}}}}$$

Medium modifications of the Delta

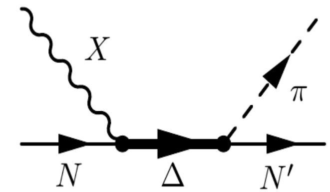

$$\boxed{-\Im(\Sigma_\Delta) = C_{QE}\,(\rho/\rho_0)^\alpha + C_{A2}\,(\rho/\rho_0)^\beta + C_{A3}\,(\rho/\rho_0)^\gamma}$$

Each contribution corresponds to a different process:

- QE $\Longrightarrow \Delta N \to \pi NN$ (still one pion in the final state)
- A2 $\Longrightarrow \Delta N \to NN$ (no pions in the final state)
- A3 $\Longrightarrow \Delta NN \to NNN$ (no pions in the final state)

We modify the free Delta decay constant to take into account the E-dependent medium modification of the Delta-width

$$\Gamma^\alpha_{\Delta\pi N} = \frac{f_{\pi N\Delta}}{m_\pi} P^\alpha_\pi$$

$$f^{\text{in-medium}}_{\Delta\pi N}(W) = f_{\Delta\pi N}\sqrt{\frac{\Gamma_{\text{Pauli}} + 2C_{QE}\,(\rho/\rho_0)^\alpha}{\Gamma^{\text{free}}_{\text{width}}}}$$

References: [*] E. Oset and L. L. Salcedo, Nucl. Phys. A 468, 631 (1987).

Interferences

$$J^{\nu} = \langle J^{\nu}_{\Delta P} \rangle + \langle J^{\nu}_{C\Delta P} \rangle + \langle J^{\nu}_{CT,V} \rangle + \langle J^{\nu}_{CT,A} \rangle + \langle J^{\nu}_{NP} \rangle + \langle J^{\nu}_{CNP} \rangle + \langle J^{\nu}_{PF} \rangle + \langle J^{\nu}_{PP} \rangle$$

PHYSICAL REVIEW D **93,** 014016 (2016)

Watson's theorem and the $N\Delta(1232)$ axial transition

L. Alvarez-Ruso,[1] E. Hernández,[2] J. Nieves,[1] and M. J. Vicente Vacas[3]

We present a new determination of the $N\Delta$ axial form factors from neutrino induced pion production data. For this purpose, the model of Hernandez *et al.* [Phys. Rev. D 76, 033005 (2007)] is improved by partially restoring unitarity. This is accomplished by imposing Watson's theorem on the dominant vector and axial multipoles. As a consequence, a larger $C_5^A(0)$, in good agreement with the prediction from the off-diagonal Goldberger-Treiman relation, is now obtained.

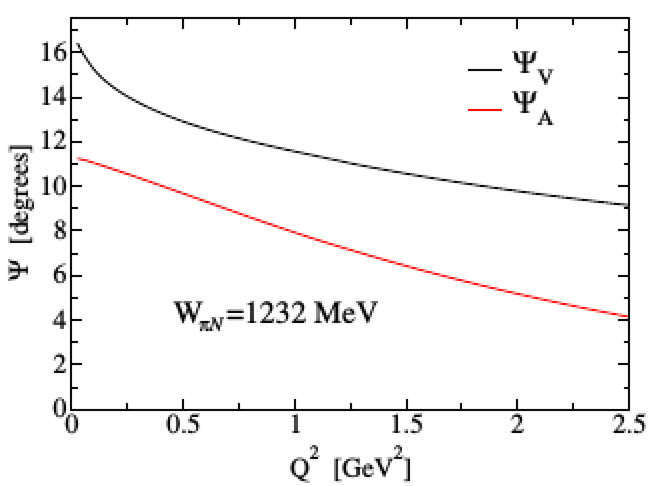

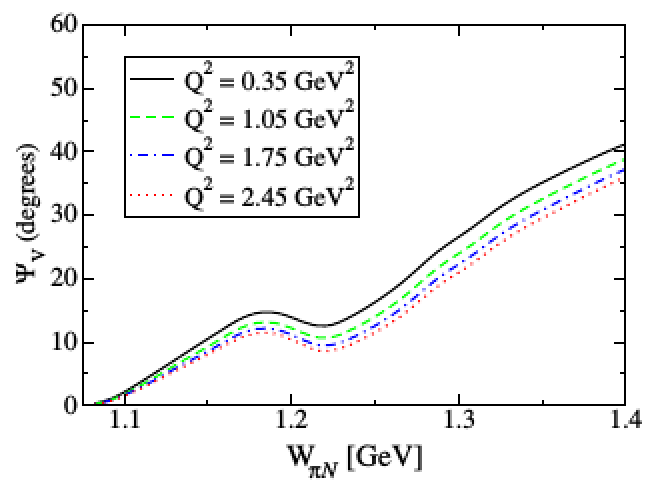

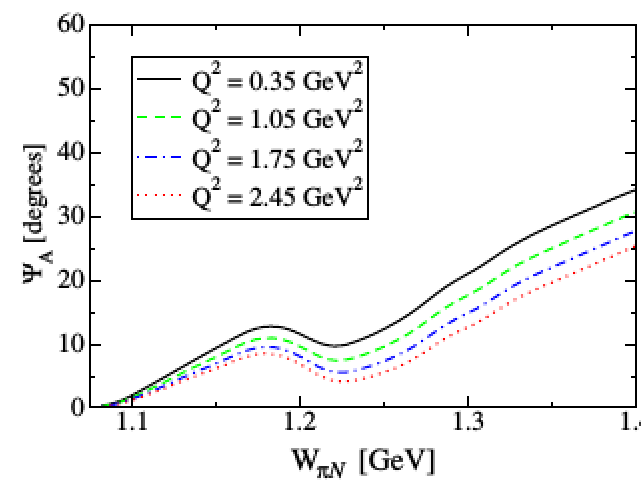

Other results

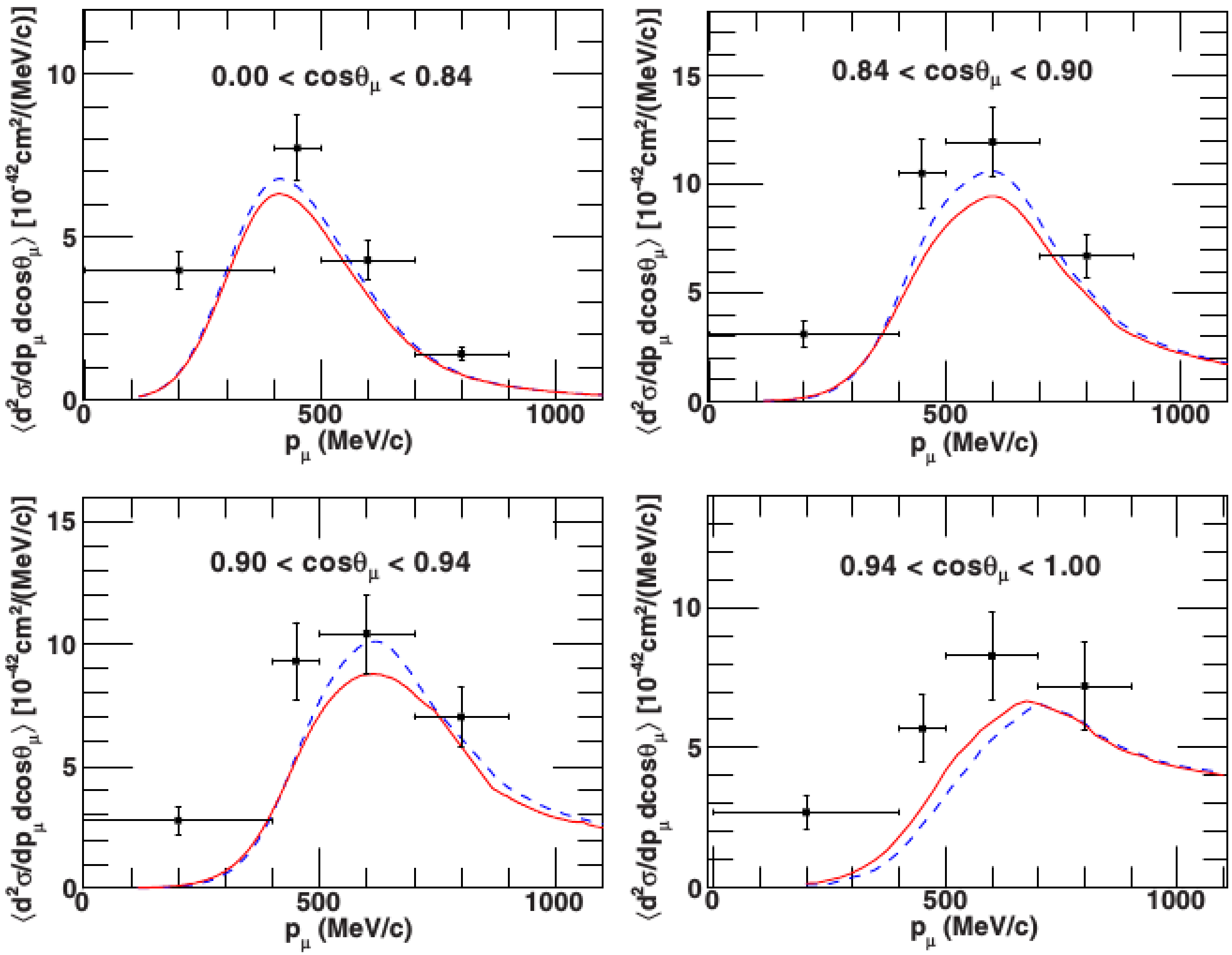

HF vs CRPA

FIG. 5. T2K flux-folded inclusive CC double-differential cross sections per target nucleon on ^{12}C plotted as a function of muon momentum p_μ, for different bins of $\cos\theta_\mu$. CRPA (solid curves) and HF (dashed-curves) are compared with T2K measurements of [12].

The Problem

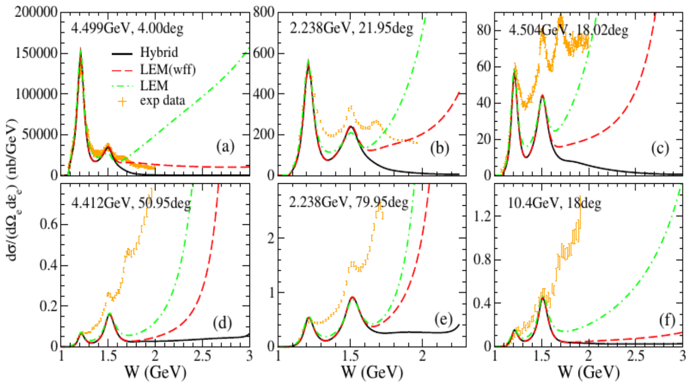

The pathologies come from the

resonances and **background terms**

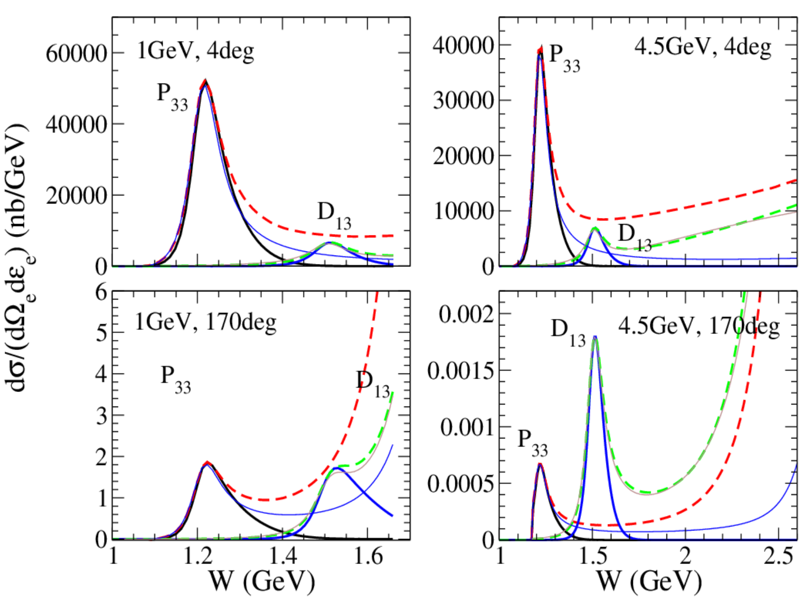

Electron scattering

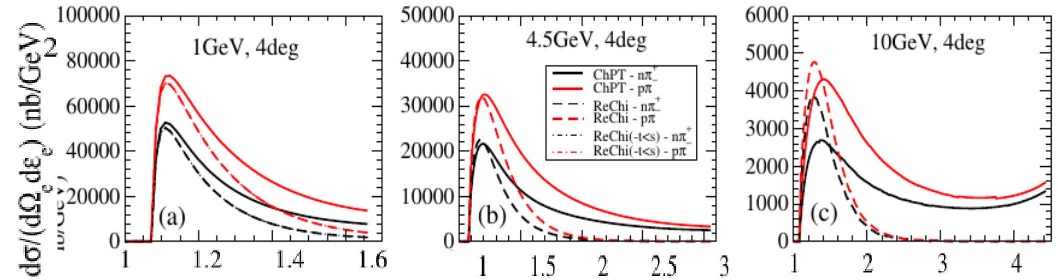

WNC neutrino scattering

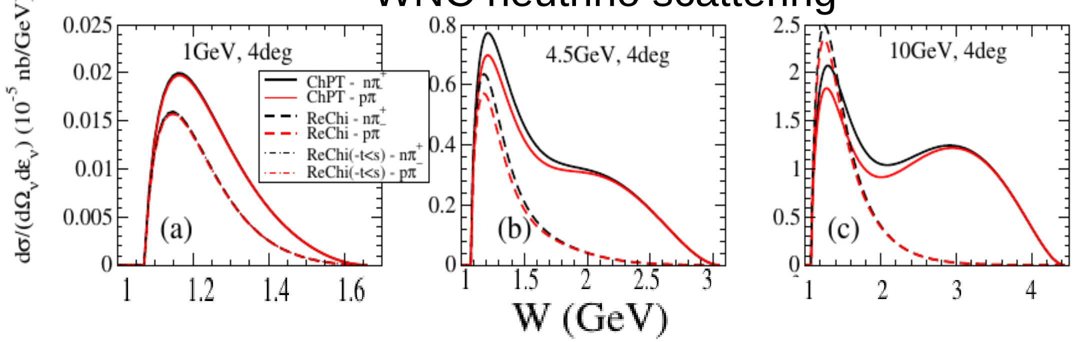

Why does this happen?

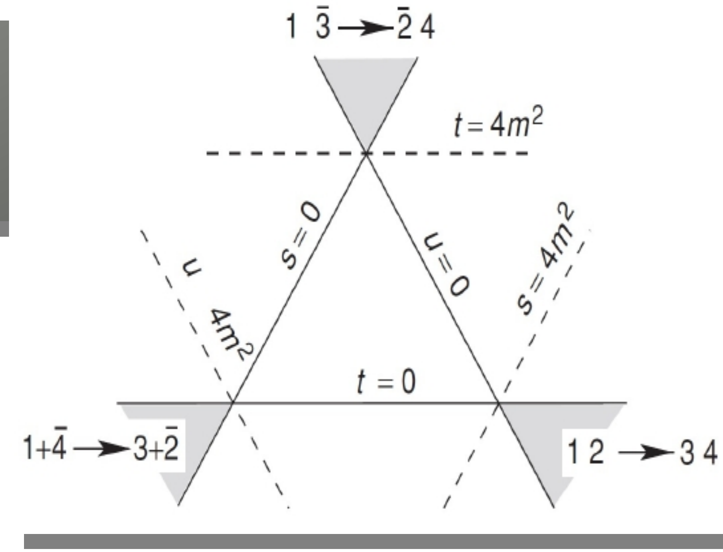

Cross channels: 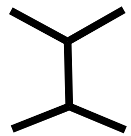

$$\mathcal{A}(t,s) = \sum_{\ell} (2\ell+1)\ A_\ell(t)\ P_\ell(z_t)$$

$$P_\ell(z_t) \xrightarrow{s\to\infty} (2s)^\ell$$

$$z_t \equiv \cos\theta_t = 1 + \frac{2s}{t-4m^2}$$

Direct channels: 

$$\mathcal{A}(s,t) = \sum_{\ell} (2\ell+1)\ A_\ell(s)\ P_\ell(z_s)$$

$$z_s \equiv \cos\theta_s = 1 + \frac{2t}{s-4m^2}$$

$$A_\ell(s) \sim \left(\frac{s-4m^2}{2}\right)^\ell$$

Behavior at threshold (barrier factor).
Feynman diagrams provide the right behavior at threshold but not at high s

Regge Theory

Based on unitarity, causality and crossing symmetry, Regge Theory predicts the following **high energy ($s \to \infty$) behavior** for the invariant amplitude:

$$A(s,t) \sim \beta(t)\, s^{\alpha(t)}$$

Regge theory does not predict the **t-dependence** of the amplitude.

For that, one needs a model.

$\alpha(t)$: Families or Regge trajectories

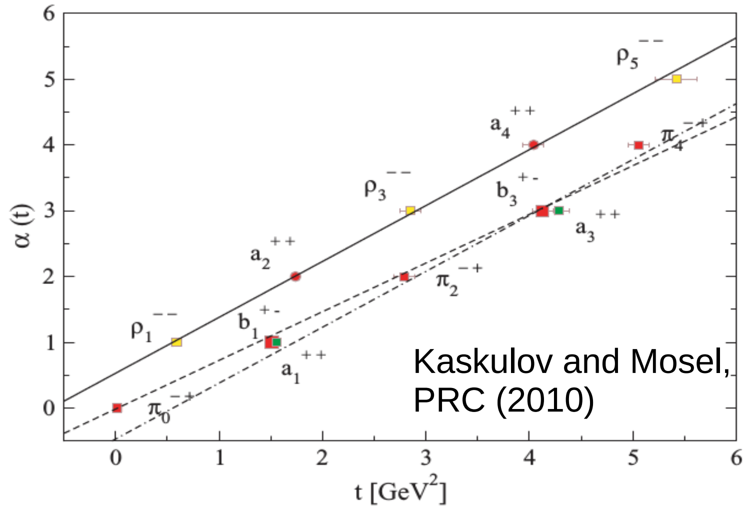

Kaskulov and Mosel, PRC (2010)

Regge Theory

$$\mathcal{A}(t,s) = \sum_{\ell} (2\ell + 1)\, A_\ell(t)\, P_\ell(z_t)$$

$$z_t \equiv \cos\theta_t = 1 + \frac{2s}{t - 4m^2}$$

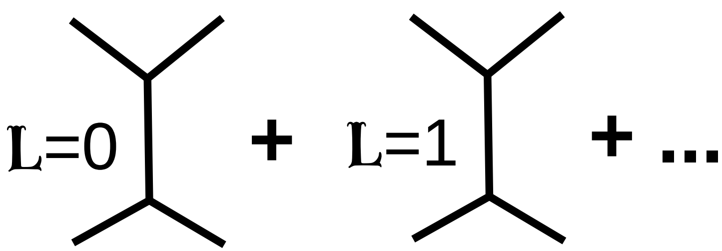

$$\frac{\lambda^2}{m^2 - t}$$

$$P_\ell(z_t) \xrightarrow{s\to\infty} (2s)^\ell$$

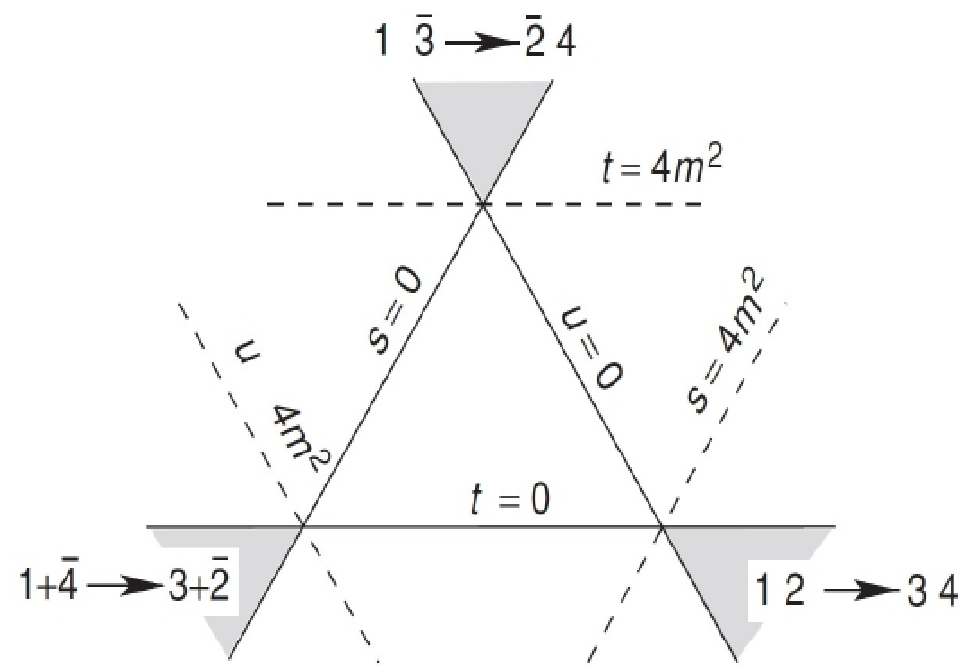

Regge Theory

$$\mathcal{M}(s,t) = -\frac{1}{2i}\oint_{C_1} d\lambda \frac{(2\lambda+1)\,\mathcal{M}_\lambda(t)\,P_\lambda(-\cos\theta_t)}{\sin(\pi\lambda)}$$

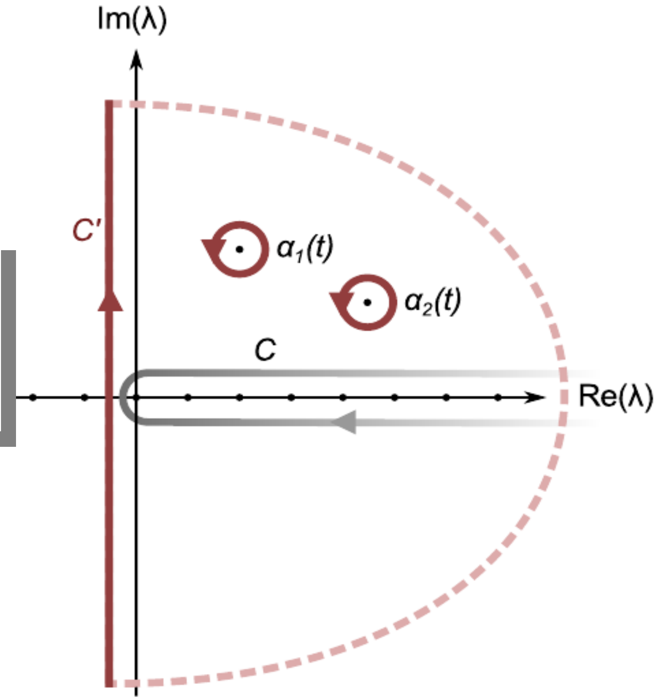

$$\mathcal{M}^{\zeta}_{\mathrm{Regge}}(s,t) = C\sum_i \left(\frac{s}{s_0}\right)^{\alpha_i^{\zeta}(t)} \frac{\beta_i^{\zeta}(t)}{\sin\left(\pi\alpha_i^{\zeta}(t)\right)} \frac{1+\zeta e^{-i\pi\alpha_i^{\zeta}(t)}}{2} \frac{1}{\Gamma\left(\alpha_i^{\zeta}(t)+1\right)} .$$

High-energy model: results

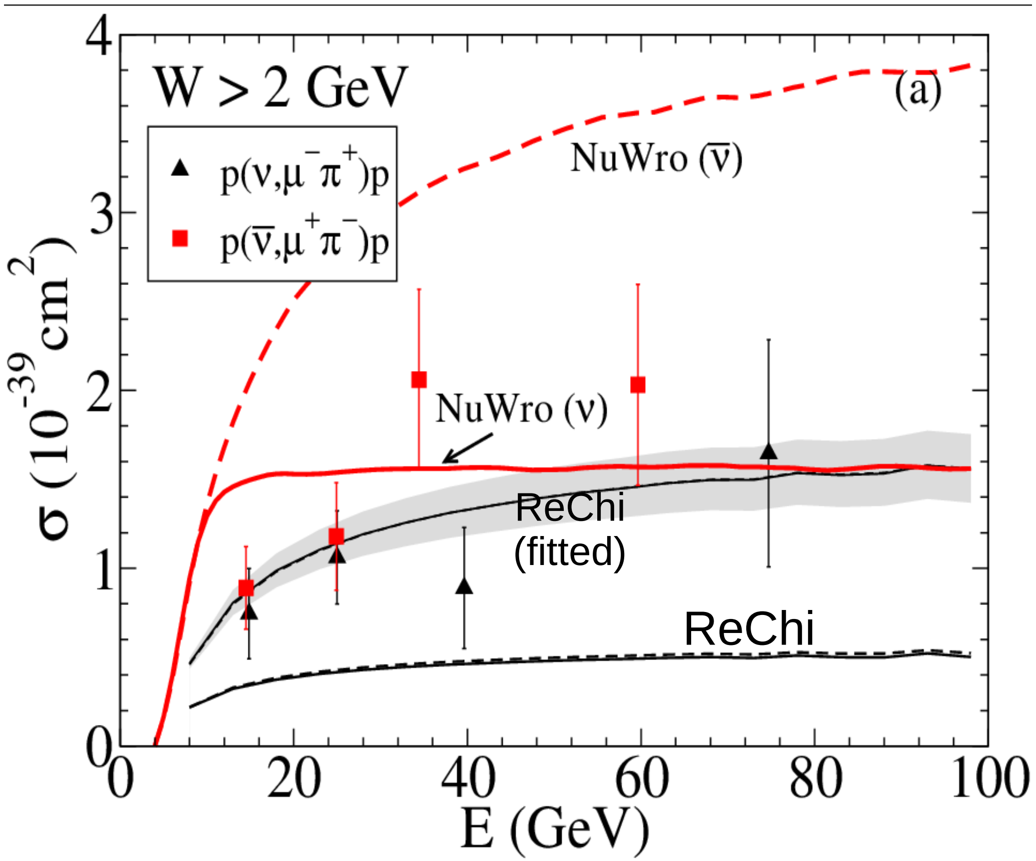

Figure: ReChi model and NuWro predictions are compared with high energy cross section data for neutrino and antineutrino reactions (Note the high energy cut W>2 GeV !!). Data from Allen et al. NPB264, 221 (1986).

ReChi model: One free parameter in the boson-nucleon-nucleon vertex

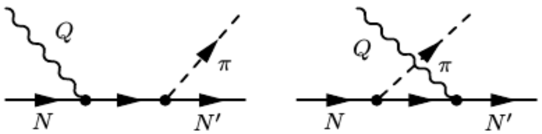

$$G_A[Q^2, s(u)] = g_A \left(1 + \frac{Q^2}{\Lambda_{Apn^*}[s(u)]^2}\right)^{-2}$$

$$\Lambda_{Anp^*}(s) = \Lambda_{Apn} + (\Lambda^A_\infty - \Lambda_{Apn})\left(1 - \frac{M^2}{s}\right)$$

$\Lambda^A_\infty = (7.20 \pm ^{2.09}_{1.32})$ GeV !!!

NuWro: Based on DIS formalism and PYTHIA for hadronization.

Antineutrino cross section is ~2 the neutrino one:

$$\bar\nu + \overbrace{uud}^{p} \to \mu^+ + \overbrace{\bar u d}^{\pi^-} + uud\,,$$
$$\nu + uud \to \mu^- + \underbrace{u\bar d}_{\pi^+} + uud\,.$$

Hybrid model

1) Regularizing the behavior of resonances (u- and s-channel contributions): we multiply the resonance amplitude by a dipole-Gaussian form factor

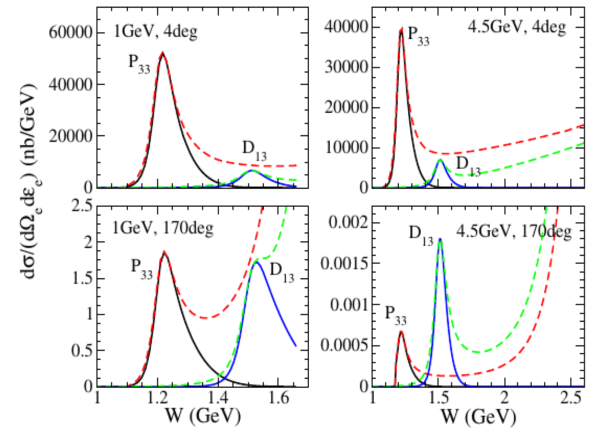

$$F(s,u) = F(s) + F(u) - F(s)F(u)$$

$$F(s) = \exp\left(\frac{-(s-M_R^2)^2}{\lambda_R^4}\right) \frac{\lambda_R^4}{(s-M_R^2)^2+\lambda_R^4}$$

2) Gradually replacing the ChPT background by the High-energy (ReChi) model: we use a phenomenological transition function

$$\widetilde{\mathcal{O}} = \cos^2\phi(W)\mathcal{O}_{ChPT} + \sin^2\phi(W)\mathcal{O}_{ReChi}$$

$$\phi(W) = \frac{\pi}{2}\left(1 - \frac{1}{1+\exp\left[\frac{W-W_0}{L}\right]}\right), \quad \begin{aligned} W_0 &= 1.7\ \text{GeV} \\ L &= 100\ \text{MeV} \end{aligned}$$